Geoderma 232–234 (2014) 219–235

Contents lists available at ScienceDirect

Geoderma

journal homepage: www.elsevier.com/locate/geoderma

The evolution of Mediterranean wetlands in the first millennium AD: The case of Les Arenes floodplain (Tortosa, NE Spain)

Arnald Puy [a,*], Andrea L. Balbo [a], Antoni Virgili [b], Helena Kirchner [b]

[a] Complexity and Socio-Ecological Dynamics (CaSEs), Department of Archaeology and Anthropology, Institució Milà i Fontanals, Consejo Superior de Investigaciones Científicas (IMF-CSIC), C/Egipcíaques 15, Barcelona 08001, Spain

[b] Arqueologia Agrària de l'Edat Mitjana (ARAEM), Departament de Ciències de l'Antiguitat i l'Edat Mitjana, Facultat de Filosofia i Lletres, Universitat Autònoma de Barcelona (UAB), Campus de Bellaterra s/n, Cerdanyola 08193, Spain

ARTICLE INFO

Article history:
Received 21 February 2014
Received in revised form 27 April 2014
Accepted 2 May 2014
Available online 2 June 2014

Keywords:
Geoarchaeology
Wetlands
Palaeosoils
Palaeoclimate
Mediterranean
Al-Andalus

ABSTRACT

Mediterranean wetlands are characterised by two factors: (1) a remarkable seasonal fluctuation in the water table and (2) a long history of anthropisation. Being exceptional archives for palaeoenvironmental and archaeological research, humid areas have been thoroughly studied to assess the interplay between people and the environment during the Holocene. We present here the study of a sedimentary sequence from a Mediterranean wetland: the Les Arenes floodplain (Tortosa, NE Spain). Fully dry to date, Les Arenes is documented as a partially drained floodplain in the 12th century records. With the aim of assessing the climatic and anthropic contribution to its desiccation, we report here the results of bulk sediment analyses, environmental magnetism, soil micromorphology and AMS dating of this sedimentary sequence, plus a review of the available historical records. The outcome is a clearer understanding of the evolution of this Mediterranean floodplain during the 1st millennium AD, which implications may be extrapolated to other floodplain wetlands in the Iberian Peninsula and the Mediterranean. Wet conditions and a low to medium-energy depositional environment are attested in Les Arenes between the 1st and 7th centuries coinciding with the Iberian-Roman Humid Period (IRHP) and the Dark Age Humid Period (DAHP). Drier conditions between the 7th and 10th centuries concur with enhanced fluvial dynamics, the Medieval Climate Anomaly (MCA) and the first arrival of Arabic-Berber populations in the Iberian Peninsula (al-Andalus, starting in AD 711). Results suggest that although the shift from wet to dry conditions in Les Arenes complies with major climatic trends, the construction of the first drainage canals by Arab-Berber groups likely contributed to the enhancement of on-going climate-related environmental processes.

1. Introduction

Mediterranean wetlands include deltas, coastal lagoons, permanent and temporary marshes, floodplains, lakes, *poljes*, *salinas*, oases, *chotts* and *sebkhas* (Papayannis and Salathé, 1999). In spite of their heterogeneous hydrology, edaphology, biology and topography, all wetlands share a dynamic character implying the seasonal succession of dry and humid periods. The water table rises and descends cyclically leading to a regular seasonal fluctuation in biota between aquatic and terrestrial-dominated ecosystems. This dynamic dimension of Mediterranean wetlands has been extensively exploited by humans throughout history: e.g. collection of diverse plant and animal species at different times of the year; agricultural exploitation of clayey and humid soils after drainage or retreat of the waterline; grazing areas for livestock; or in the case of coastal areas, for sailing and fishing (Balbo, 2008; Horden and Purcell, 2000). Their sensitivity to climatic shifts and continued history of anthropisation makes Mediterranean wetlands one of the best environmental sources to study the evolution of past socio-ecological dynamics.

Several studies in the Mediterranean basin have used palaeoenvironmental records to assess the interplay between climate and humans and its effects on wetlands during the Holocene, for example in Spain (Dorado Valiño et al., 2002; Gil García et al., 2006; Jiménez-Moreno and Anderson, 2012; Ruiz-Zapata et al., 2010), France (Lespez et al., 2010; Save et al., 2012; Verdin et al., 2001), Italy (Amorosi et al., 2013; Guido et al., 2013 and references therein for wetlands in Liguria, NW Italy), Greece (van Andel and Runnels, 2005; Vött et al., 2006; Zangger, 1991), Tunis (Faust et al., 2004), Turkey (Vermoere et al., 2002), Croatia (Balbo, 2008; Balbo et al., 2006) or Slovenia (Budja and Mlekuz, 2010). Most works agree that environmental changes attested during the first half of the Holocene were mostly climate-driven, while those occurring during the late Holocene were highly amplified by the human factor (Balbo et al., 2006; Giraudi et al., 2011; Jalut et al., 2000, 2009). Oscillations in the extension and variety of most Mediterranean wetlands followed major climatic trends until c. 5 ka BP (coinciding approximately

* Corresponding author. Tel.: +34 93 442 34 89; fax: +34 93 443 00 71.
E-mail addresses: arnald.puy@gmail.com (A. Puy), balbo@imf.csic.es (A.L. Balbo), antoni.virgili@uab.cat (A. Virgili), helena.kirchner@uab.cat (H. Kirchner).

http://dx.doi.org/10.1016/j.geoderma.2014.05.001
0016-7061/

with the beginning of the European Iron Age). The steady decrease in humid areas detected in later periods has been related to an increase in agriculture, grazing, irrigation, drainage and related sediment transport processes, i.e. soil erosion and siltation of water bodies (Balbo, 2008; Broothaerts et al., 2013; Gurnell and Petts, 2002; Roberts et al., 2001). The last 2000 years are especially well suited to study the interplay between humans and climate for the evolution of Mediterranean humid areas, since palaeoenvironmental information can be contrasted with historical records (Cacho et al., 2010).

In this paper we present the geoarchaeological study of a sediment column from the floodplain of Les Arenes, in Tortosa, NE Spain, during the 1st millennium AD. Les Arenes is located 10 km NW of the Ebro Delta, one of the most important and ecologically rich wetlands of the Iberian Peninsula (Ibáñez and Prat, 2003). Les Arenes is currently dry, although the 12th century documents refer to it as a partially drained and cultivated floodplain (Virgili, 2010). In that sense, the targets of our research were: 1) to characterise the floodplain previous to the first attested drainage; 2) to identify and date the main shift from wet to dry conditions; and 3) to provide the socio-ecological context of this environmental change. Such information is not only relevant to understand the different processes that led to the disappearance of Mediterranean wetlands, but also in support of initiatives aiming at their recovery, protection and conservation (Daoud-Bouattour et al., 2011). Moreover, our study has implications for the overall assessment of climatic trends in the Iberian Peninsula and the Mediterranean during the first millennium AD, including the Iberian-Roman Humid Period (IRHP); the Dark Ages Humid Period (DAHP) and the Medieval Climate Anomaly (MCA) (Cacho et al., 2010; Moreno et al., 2012; Nieto-Moreno et al., 2011), as well as for the appraisal of the agricultural and landscape changes fostered in the Iberian Peninsula (al-Andalus) after the arrival of several Arabic-Berber tribes and clans in AD 711 (Barceló, 2001; Barceló et al., 1995; Glick and Kirchner, 2000; Sitjes, 2006).

1.1. Physical context

The Les Arenes floodplain is located inside a meander near the mouth of the Ebro River (0° 30′ 48″, 40° 47′ 31″), S of Tortosa, NE Spain (Fig. 1, image A). The floodplain is made of Holocene silt and sand deposits and extends over approximately 350 ha. The surface topography has a low gradient and is slightly convex, with the terrain gently sloping away from the riverbank towards the valley sides. The channel banks and levées are slightly higher than the flood basin, where ridge/swale landforms and scroll-bars that have formed during successive river migrations are still visible. Five different torrents, which have been mostly concealed in the 20th century to reduce damage in case of torrent overflow, cross the floodplain from E to W.

The local geology consists of Quaternary mountain ranges made of sandy-silty calcareous red gravels and blocks of quartzite, mudstone, marlstone, schist, Mesozoic calcareous boulders and limestone with alveolites (Arasa Tuliesa, 1994). The local climate is characterised by annual average temperatures ranging between 15.5 °C and 17 °C (10 °C in winter, 22 °C in summer). Annual precipitation, concentrated in spring and autumn, fluctuates between 500 and 600 mm (Agenda 21, 2009). Potential evapotranspiration amounts to 712–855 mm and hydric deficit to 200–300 mm (Rigola, 2011). According to Thornthwaite's index (1948), these features correspond to a semi-arid climate.

The soils in Les Arenes are calcareous Fluvisols and Luvisols (FAO, 2006) and are for the most part planted with *Citrus sinensis*, other fruit trees and cereals. Herbaceous crops, which require more humidity, are located closer to the river. Mediterranean and Sub-Mediterranean forests predominate in the surrounding slopes, including *Chamaerops humilis*, *Pistacea lentiscus*, *Olea europea* var. *sylvestris*, *Rosmarinus officinalis* and *Globularia alypum* (Agenda 21, 2009).

The Agència Catalana de l'Aigua (Catalan Water Agency) classifies Les Arenes as prone to total flooding within a 50-year frequency period. Historical inundations attested in local written records between AD 1355 and 1982 include 40 overbank floods (i.e. mean of one flood every 15 years): 17 were classified as catastrophic (implying destruction of crops, agricultural fields and civil infrastructures) and 23 as extraordinary (implying temporary disruption in day-to-day activities) (Taylor et al., 2006; Vallve and Martin-Vide, 1998). The systematic construction of dams and reservoirs along the course of the Ebro and its tributaries has significantly reduced the frequency of the floods from the 20th century onwards (Batalla et al., 2008). The Ebro River, 930 km long, is presently regulated by 187 dams, most of them built after 1950 (Batalla et al., 2004). These structures have interrupted the sedimentary flow along the channel, with significant effects on the ecosystems of the lower course of the river and its annual average discharge (Vericat and Batalla, 2006). Magdaleno et al. (2012), for example, observed that in the early 20th century the Ebro still preserved areas with large sediment bars, in-channel bar islands and broad riparian forests. These landforms associated with river floodplains have currently disappeared, but were still perfectly visible in Les Arenes in 1927 (Fig. 1, images B–C). Regarding river flow, the historical data from the Tortosa gauging station compiled by the Ministerio de Agricultura, Alimentación y Medio Ambiente (Ministry of Agriculture, Alimentation and Environment) of Spain shows that the Ebro annual average discharge fell from 16,244.8 hm^3 per year between 1912 and 1964 to 9472.3 hm^3 per year between 1973 and 2010 (Anuario de Aforos, 2010). Current annual discharge ratio averages to 9540.1 hm^3, January and October being the months with the highest and lowest values (1596.85 hm^3 and 337.37 hm^3 respectively).

No palaeogeographical studies have been published to our knowledge in this stretch of the Ebro River. The first fieldwork and photointerpretation aiming at understanding recent landscape evolution and documenting relict drainage canals in Les Arenes was undertaken in 2011 within the framework of research projects directed by H. Kirchner and A. Virgili. The 1927 aerial imagery shows the Ebro meander bend in Les Arenes running 500 m further east compared to the current river course (Fig. 1, images B–C). The riverbank in 1927 coincides with a relict drainage canal attested during fieldwork and built after the second third of the 20th century to gain parcels of agricultural land westwards. The eastern limit of the area that undergoes flooding with a 10-year frequency is also aligned with relict drainage canals that have now been converted into pathways stretching N–S along the floodplain (Fig. 1, image A). Agricultural plots located within this floodable area display an elongated profile in the aerial images, standing in sharp contrast with plots located eastwards. From these features we deduce that the current river course in Les Arenes has resulted from a progressive westwards migration of the meander bend due to: (1) fluvial and geomorphological processes causing the erosion of the outer bank, sediment deposition at the inner side of the bend and lateral extension of the meander bend, as well as (2) anthropic influences including the construction of drainage canals and the reclamation of wet soils and palaeochannels for agriculture.

1.2. Historical context

The city of Tortosa and its surrounding area are mentioned in texts referring to the onset of the Andalusi period (AD 711–1148) (Bramon, 2002), which was characterised by the arrival of Arabic-Berber tribes and clans in the Iberian Peninsula (al-Andalus) (Barceló, 1999; Barceló and Kirchner, 1992). The first systematic written records of Tortosa and Les Arenes floodplain followed the conquest of the city and its territory by the Count of Barcelona Ramon Berenguer IV and the Genoa Republic in AD 1148, in the context of the Second Crusade (Virgili, 2001). These texts were commissioned by the new Christian lords to formally sanction the new social order. The properties subtracted from the former Andalusi inhabitants were re-distributed, and their owners were subjected, deported or enslaved. In these texts, the lands immediately to the S of Tortosa were mostly defined as *terrae*, *campi* (both referring to lands with cereal crops) and *vineae* (a generic term referring to

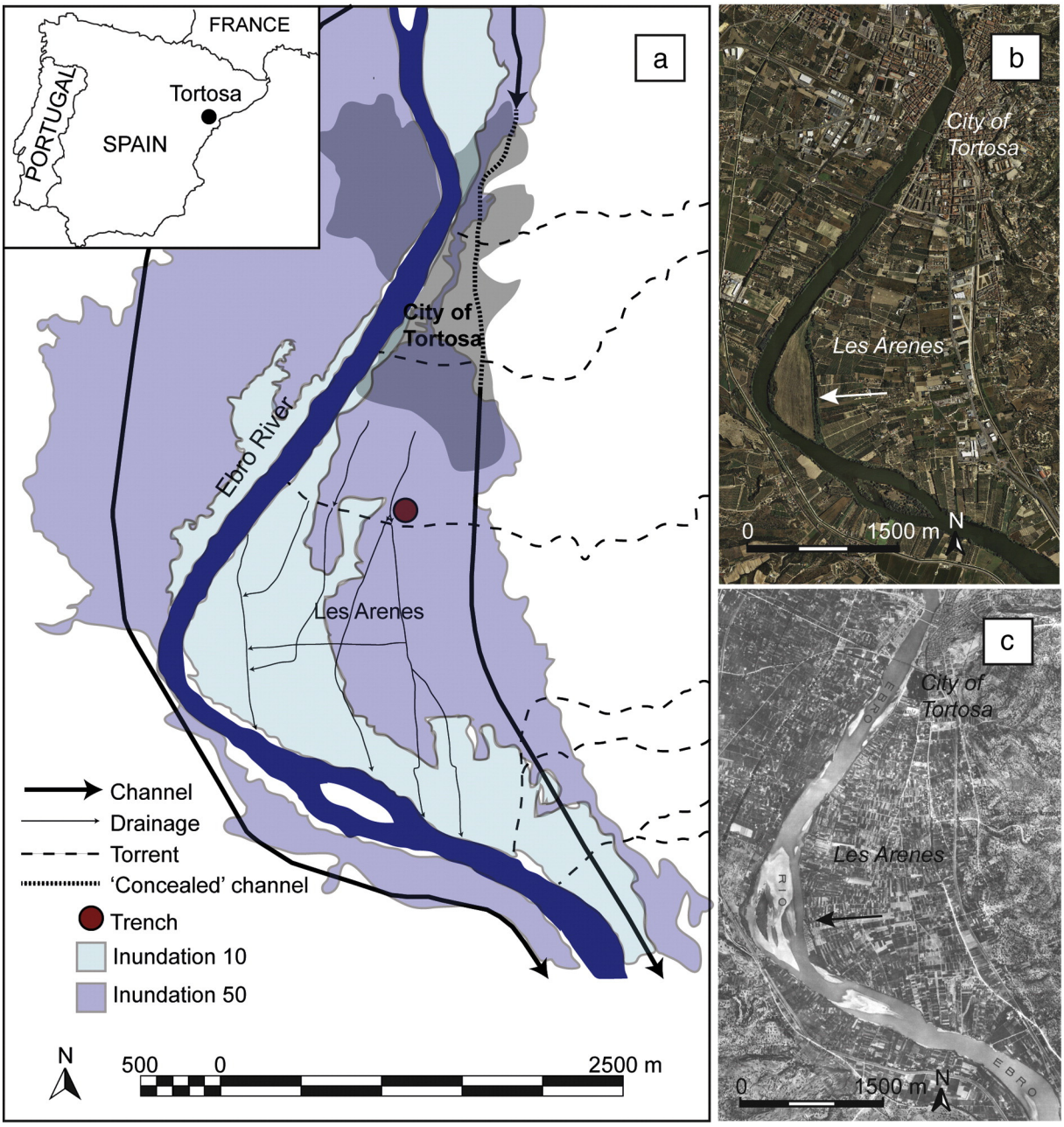

Fig. 1. Location and evolution of Les Arenes floodplain. a) Map showing the location of the trench and inundation areas, within a 10 years frequency period (light blue) and 50 years frequency period (dark blue). Inundability data comes from Agència Catalana de l'Aigua, Divisió de Sistemes d'Informació, sheets 497 and 522. Thin black arrows indicate the path of relict drainage canals identified after fieldwork (research project directed by H.Kirchner and A.Virgili). The black area indicates the extension of the city of Tortosa. b) Orthofoto taken in 2007 and available in the Institut Cartogràfic Català (ICC) webpage. c) Aerial photograph taken in 1927 by CETFA (Compañía Española de Trabajos Fotogramétricos Aéreos) and available in the Confederación Hidrográfica del Ebro webpage. The presence of point, transverse and mid-channel bars, landforms typically associated with dynamic meandering rivers and their floodplains, indicated the still existing ecological connection between the river Ebro and its floodplain by the early 20th century. The arrow indicates the last stage of land reclamation through drainage, fully consolidated in 2007 but still pending in 1927.

vineyards), with minor references to *horti* (orchards). Further S the landscape was described as a *pratum*, a term referring to humid marshy areas. Documents dated to immediately after the feudal conquest also mention numerous canals in Les Arenes, built to drain water accumulated in the rainy season (Virgili, 2010). This historical information was taken as an *ante quem* marker for the first drainage of the floodplain. Following the data acquired after photographical and geomorphological analysis, we propose a general E to W trend for the progressive reclamation of land and stabilisation of wet soils in Les Arenes. We assume that the earliest draining took place in the easternmost portion of the floodplain at some point before the conquest by Catalan feudal lords (AD 1148). The geoarchaeological investigation presented below aim at understanding the evolution of Les Arenes during the 1st millennium AD and at relating the attested environmental changes to their socio-ecological contexts.

2. Materials and methods

2.1. Sampling

A trench (4 × 7 × 5.10 m) was excavated with a mechanical digger in an uncultivated plot located within the area identified as the earliest drained portion of Les Arenes (0° 31′ 02″, 40° 47′ 49″) (Fig. 1, image A). The resulting section was drawn and described following

Hodgson (1976). Textures of the identified layers were described as sandy clay, silty clay, silty loam, sandy silt loam and loamy sand. A moderately to well-developed palaeosoil and a weakly developed palaeosoil were identified between 305 and 290 cm and 260 and 242 cm below the current surface. Sediment samples for physico-chemical analyses (Loss on Ignition—LOI; Particle Size Distribution—PSD; Magnetic Susceptibility—Mag Sus; Anhysteretic Remanent Magnetization—ARM, Isothermal Remanent Magnetization—IRM) and Powder X-ray Diffraction (PXRD) (Evans and Heller, 1991; Heiri et al., 2001; Schmidt, 2007; Schreiner et al., 2004; Syvitski, 1991) were collected at 10 cm intervals. The transition between key layers was sampled with Kubiena boxes (4 × 20 cm) for the production of thin sections (20 μm thick) for micromorphological analysis (Benyarku and Stoops, 2005; Courty et al., 1989). Three discrete sediment samples were taken (330–360; 260–285; and 220–240 cm below the surface) for radiocarbon dating by Accelerator Mass Spectrometry (AMS). The sampling was restricted to a portion of the stratigraphic profile (between 380 and 140 cm below the surface) since the main aim of the study was to characterise the floodplain prior to the 12th century. Previous archaeological and geological work in the Tortosa area has located the 10th–12th century layers c. 200 cm below the current surface (Joan Martínez, personal communication).

2.2. Physico-chemical analyses

LOI was done by burning the samples for 4 h at 105 °C, 400 °C, 480 °C and 950 °C in order to estimate the proportion of water, organic matter, coal and calcium carbonate respectively. PSD was carried out by introducing 0.4 g sediment samples — previously treated with H_2O_2 at 10% solution to dissolve sodium polyphosphates — in a Coulter LS®. The values in microns (μm) were converted into phi (φ) units following Krumbein (1938). The description of grain size distribution followed the terminology in Friedman and Sanders (1978) and the statistical calculations were carried out after the logarithmic method described in Folk and Ward (1957). LOI was used as proxy to precise the alternation between humid and dry conditions and PSD as proxy to identify depositional dynamics.

Magnetic analyses (Mag Sus, ARM, IRM) were carried out on 10 cm^3 whole sediment samples previously dried for 6 h at 105 °C. Mag Sus was calculated with a Kappabridge KLY-2® (Geofyzica Brno; field of 0.1 mT at a frequency of 470 Hz). ARM and IRM were estimated with a superconducting rock magnetometer SRM755R® (2G Enterprises, background noise below 7×10^{-6} A/m), an alternating field demagnetiser D-Tech 2000® (ASC Scientific; applied fields: AF 100 mT with 0.005 decrease and a direct field intensity of 0.05 mT); and a pulse magnetizer IM10-30® (ASC Scientific; applied fields: 0.1, 0.3 and 1.2 T). Hard Isothermal Remanent Magnetization (HIRM) was defined as $IRM_{1.2\ T} - IRM_{0.1\ T}$; and *S*-$Ratio_{0.3\ T}$ as $IRM_{0.3\ T}/IRM_{1.2\ T}$. Mag Sus was used as proxy for the concentration of magnetic minerals; ARM as proxy for the concentration of ferrimagnetic minerals, such as magnetite and maghemite (Maher, 1986); HIRM as proxy for the absolute concentration of high coercivity antiferromagnetic minerals, such as haematite and goethite (Dalan and Banerjee, 1998; Liu et al., 2007), and the *S*-$Ratio_{0.3\ T}$ as proxy for the evaluation of variations in the relative abundance of ferrimagnetic and antiferromagnetic minerals (Dalan and Banerjee, 1998; Liu et al., 2012).

2.3. Powder X-ray diffraction

Samples were back-loaded into standard holders. Patterns were collected at room temperature using a Philips X'Pert diffractometer equipped with a θ/2θ goniometer and operating at 50 kV and 40 mA. Cu Kα radiation (λ = 1.5419 Å) was used. Data were collected in the range 5–60° of 2θ using a continuous-scan technique with a step size of 0.03° of 2θ and a time per step of 1 s. PXRD was used as proxy to identify the mineralogy and sources of the sedimentary material.

2.4. Soil micromorphology

Thin sections were prepared at SCT Micromorfologia de Sòls i Anàlisis d'Imatges Laboratory, Universitat de Lleida, Spain. After drying for two months at room temperature, the sediments collected in the Kubiena boxes were impregnated with Palatal polyester with styrene (100–200 ml/L), MEK (5–7 ml/L) and two drops of Cobalt Octoate. Following impregnation, samples were left to dry for another six weeks. After this, thin sections were cut with a diamond blade and polished with a machine Brot Tech® 1.03.12.P until a thickness of 20 μm was achieved. After preliminary observation with a petrographic microscope several layers not identified during fieldwork were detected. These units were described as microfacies and labelled with the letter identifying the layer to which they belonged and a specific number (e.g. microfacies A1). The analysis of thin sections was carried out with Leica® MZ9.5 and DM2500 microscopes, and the micromorphological description and interpretation were based on Courty et al. (1989), Stoops (2003) and Stoops et al. (2010a). Soil micromorphology was used as proxy to identify processes of soil formation, pedofeatures and sediment microstructure.

2.5. AMS dating

AMS dating was carried out at Beta Analytics® with fragments of *Olea europaea*, *Quercus ilex/coccifera* and an unidentified angiosperm found during wet sieving (0.25 mm mesh) of the sediment samples. Dates were calibrated to years BP (present 1950) and years BC/AD using Calib 6.1 (Reymer et al., 2009).

3. Results and discussion

Results obtained from fieldwork and physico-chemical analyses are shown in Fig. 2. Granulometry and grain size statistics are presented in Fig. 3. Powder patterns are shown in Fig. 4. Thin section description is summarised in Table 1. Ages obtained from radiocarbon dating are presented in Table 2.

3.1. Floodplain dynamics

3.1.1. Layer A (fine laminated deposits)

The evolution of mean grain size (from 4.7 φ to 5.5 φ) and skewness (−0.4 φ to −0.2 φ) between 380 and 330 cm (layer A) suggests a moderate and progressive decrease in the kinetic deposition energy between approximately the 1st and the 3rd centuries AD (AD 86–252, median AD 182). The presence of fine and very fine sand grains decreases significantly upwards with regard to very coarse and coarse silt grains, which become the dominant fraction (Fig. 3).

Layer A includes microfacies A1, which shows a superposition of about 20 submillimetric laminated wavy to linear beds of poorly to moderately sorted fine silt, medium silt and silty clays, including small organic particles and few vesicles (Fig. 5, image D). This is a depositional surface crust formed by deposition of fine particles at a certain distance from their original location after translocation by water (Courty et al., 1989; Valentin and Bresson, 1992). According to Courty et al. (1989) and Morin (1993), processes leading to the formation of surface crusts include flood and irrigation water, raindrop splash of loose soil particles from ridges and surrounding higher ground, overflow and floods from rivers and runoffs and sheet erosion. Almost invariably surface crusts overlie structural crusts such as that represented by the top of layer A, from which microfacies A1 is separated by a sharp boundary (Fig. 5, image D). Particle size, generally above 5 φ, and the thickness of beds (<40 μm), suggests that microfacies A1 formed by deposition of fine particles suspended in a succession of low-energy overland flows. Vesicles observed in microfacies A1 are spherical and have a diameter of less than 500 μm, suggesting they formed as air bubbles trapped in the sediment during desiccation of the crust (Bresson and Valentin, 1993;

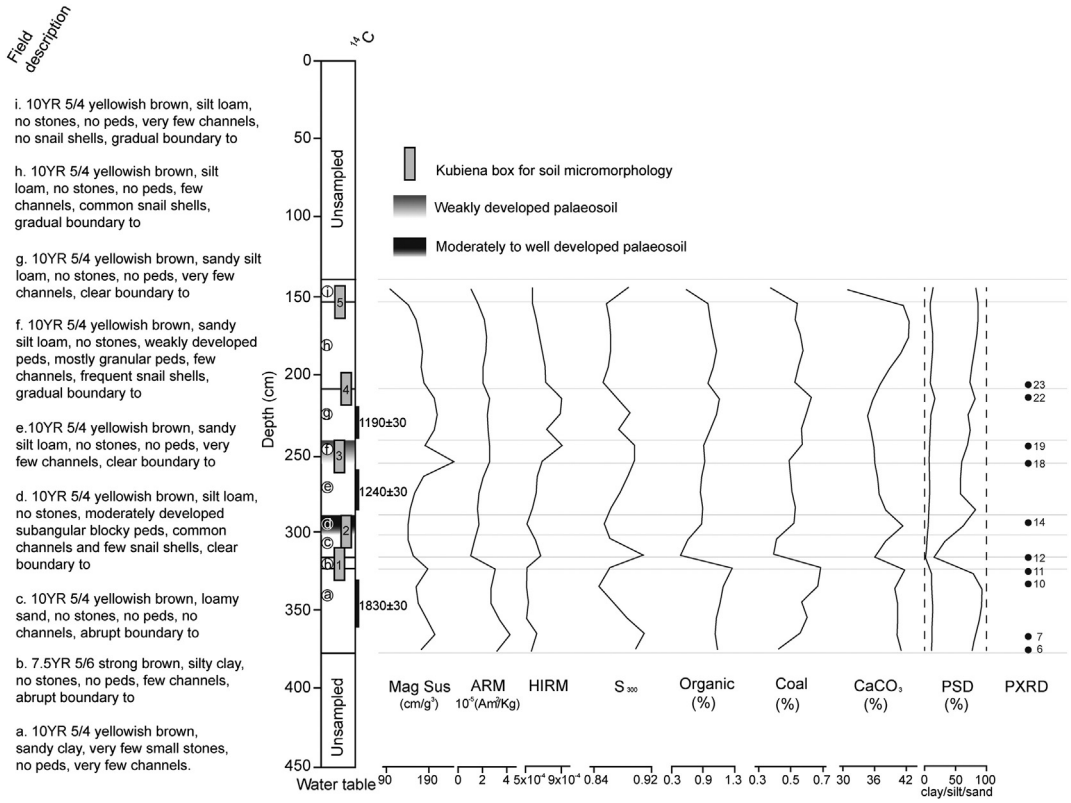

Fig. 2. Description of the section, location of the Kubiena boxes for soil micromorphology and results of physico-chemical analyses.

Stoops, 2003). It is likely that microfacies A1 was buried under layer B soon after drying: surface crusts can easily be destroyed by biological activity or human intervention, so that their preservation indicates rapid burial after formation (Courty et al., 1989).

3.1.2. Layer B (incipient Fluvisol)

Mean grain size from PSD in layer B (4.7 φ) suggests a slight increase in the energy of deposition between 330 and 320 cm (Fig. 3). However, analysis of thin sections shows that very fine and fine sand grains found in layer B are intruded from layer C through bioturbation channels (±1000 μm width and ±7000 μm length) (Fig. 5, image F). This intrusion seems responsible for the overestimation of coarse particles in layer B in the PSD test. In thin section layer B is made of a vesicular microstructure formed by up to five parallel silty clay and clayey silt laminations, with no coarse material, but with strong evidence of bioturbation by root channels and soil fauna (Fig. 5, image F). LOI data shows that layer B has the highest organic content of the whole stratigraphic profile (1.45%) and is also rich in calcium carbonate (41.69%) (Table 3). Calcium carbonate features in thin section include calcareous micromass, few micritic coatings in voids and few

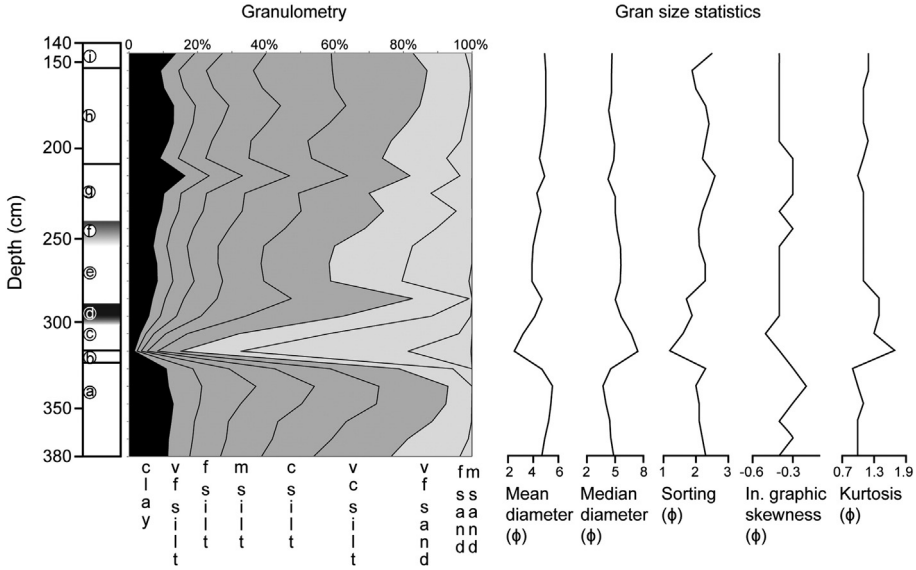

Fig. 3. Granulometry and grain size statistics of samples. See Fig. 2 for a description of the sedimentary sequence.

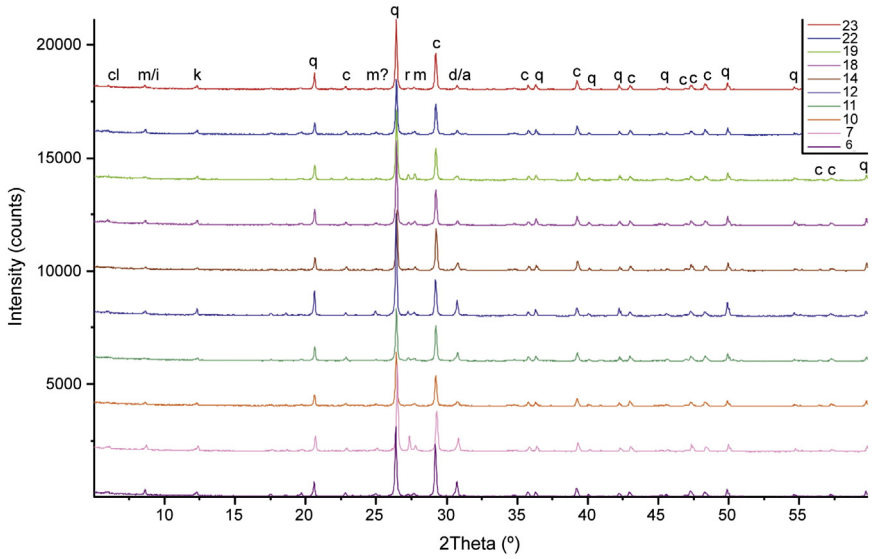

Fig. 4. Powder patterns of samples subjected to PXRD tests (see Fig. 2): cl = clinochlore; m = muscovite; i = illite; k = kaolinite; q = quartz; c = calcite; r = rutile; d = dolomite; a = ankerite.

weakly to moderately impregnated typical and aggregate irregular orthic nodules with diffuse and sharp boundaries, mostly less than 50 μm in diameter (Fig. 5, images G–H). Micritic coatings result from the precipitation of calcitic crystals in the clayey micromass (Durand et al., 2010). Calcitic orthic nodules with diffuse boundaries are generally formed in situ under conditions favouring rapid carbonate precipitation, such as frequent desiccation (Khormali et al., 2006; Stoops, 2003). Some calcium carbonate pedofeatures in layer B appear related to redoximorphic features, mostly iron/manganese diffuse nodules less than 170 μm in diameter, suggesting fluctuating high-water table (Sehgal and Stoops, 1972). Few iron quasi-coatings and typical aggregate iron nodules, usually formed under reducing conditions (Lindbo et al., 2010), were also identified in the groundmass (Fig. 5, image I). Overall features observed for layer B suggest that: (a) this is the result of several depositional events involving deposition of fine material in suspension, (b) following deposition, the sediments composing layer B underwent alternated dry and humid conditions and (c) the surface was colonised by plants and microorganisms, leading to bioturbation and the incipient development of a Fluvisol (FAO, 2006).

3.1.3. Layer C (flood event and point bar accretion)

Layer C (320 to 300 cm) is by far the coarser deposit in the whole stratigraphic profile (Fig. 3, Table 3), with a significant content of medium sand grains (18.3–3.8%). Mean grain size is fine to very fine subangular and subrounded sand (2.5 φ–3.2 φ). The kurtosis (1.7 φ; 1.3 φ) indicates that most particles are grouped within a limited size range. This homogeneity hints at a depositional environment causing a good sorting of the sediments and characterised by lower than average viscosity. Numerous subangular blocky peds less than 1000 μm in size from layer B were documented in microfacies C1, suggesting that the deposition of layer C caused the erosion and mobilisation of the surface of layer B (Fig. 5, image J). Layer C does not show bedding or microlamination, but a homogenous structure, and a clear truncation line is visible in thin sections between layers B and C (Fig. 5, images J–L). These features, together with the geomorphological data obtained after analysis of the 1927 aerial image and the floodable areas within a 10 year frequency period, suggest this deposit is a relict point bar formed following the retreat of the waterline after a lateral migration of the river during a major flood, probably at some point between AD 252 and 656.

3.1.4. Layer D (Vertisol)

In thin section, layer D has most of the vertic features enumerated by Kovda and Mermut (2010): (a) a granular structure in surface horizons (microfacies D2) and a blocky structure in the subsurface (microfacies D1), (b) slickensides and wedge-shaped peds, (c) deep, wide cracks due to shrinking and swelling, a process that causes the detachment of material from the surface to lower horizons, (d) weak horizonation, (e) iron and/or manganese oxide pedofeatures, for the most part consisting of very few medium to strongly impregnated iron typical nodules less than 120 μm in diameter, iron coatings and iron hypocoatings, (f) a clayey texture and (g) a calcite-rich groundmass with calcitic crystallitic b-fabric, a common feature of Vertisols in arid and semi-arid environments (Durand et al., 2010) (Fig. 5, images M–O). Calcium carbonate content is among the highest across the sampled profile (41.33%) (Table 3). Frequent typical weakly to moderately impregnated orthic calcium carbonate nodules with diffuse boundaries less than 1300 μm in diameter, along with common calcium carbonate hypocoatings and few calcium carbonate coatings with micritic crystals, have been identified in thin section. The most significant textural pedofeature of the Vertisol is the presence in the subsurface horizon of very few calcium carbonate hypocoatings coating iron hypocoatings, probably formed as a consequence of the transition from humid to drier edaphological conditions (Stoops et al., 2010b) (Fig. 5, image P). A small number of snail shells and calcium carbonate replaced plant tissues also suggest that biological activity took place in the surface horizon. According to FAO (2006), Vertisols are found in lower landscape positions such as dry lake bottoms, river basins, lower river terraces and other periodically wet lowlands.

3.1.5. Layer E (Vertisol burial)

The dating of the fragments of *Q. ilex/coccifera* present in layer E (AD 686–873, median AD 767) provides a maximum chronological marker for the formation and burial of the Vertisol (layer D). The mean grain size of layer E (3.9 φ, very fine sand), and its sand content (19.5% fine sand; 20.8% very fine sand) are much higher than those of the Vertisol and suggest that its deposition coincided with an increase in the energy of the sedimentary agent (Fig. 3) (Fig. 6, image F).

3.1.6. Layer F (Regosol)

A weakly developed palaeosoil was identified between 260 and 242 cm in coincidence with a significant reduction in the percentage of very fine and fine sand grains (Fig. 3). This palaeosoil shows a

Table 1
Micromorphological description of thin sections. Frequency: * = very few; ** = few; *** = common; **** = frequent; ***** = dominant; ****** = very dominant. Abbreviations for coarse material (mineral): sa = subangular; sr = subrounded; (organic): ch = charcoal. Abbreviations for micromass: cc = calcium carbonate. Abbreviations for iron pedofeatures: ty, agg = typical aggregate.

K	Depth (cm)	Layer	μfacie	Microstructure	Porosity	c/f 2 μm ratio	c/f related distribution	Mineral	Organic	Micromass	Iron pedofeatures	$CaCO_3$ pedofeatures	Observations
5	145–165	I		Complex; vughy and granular	***Vughs **channels **vesicles	19/1	Double spaced porphyric	sa, sr quartz grains (152 μm ∅)		10YR yellowish brown, cc fabric	**Nodules	**Nodules	
		H		Vughy	***Vughs ***channels ***vesicles	23/1	Double spaced porphyric	sa, sr quartz grains (156 μm ∅)		10YR yellowish brown, cc fabric	**Nodules	**Nodules	
4	198–218	H		Vughy	***Vughs ***channels ***vesicles	23/1	Double spaced porphyric	sa, sr quartz grains (<197 μm ∅)	*Iron-replaced	10YR 5/4 Yellowish brown, cc fabric	**Nodules	**Nodules	
		G		Vesicular	***Channels ***chambers ****vesicles	18/1	Double spaced and close porphyric	sa, sr quartz grains (<180 μm ∅)	**Iron-replaced	10YR 5/4 yellowish brown, cc fabric	**Nodules	**Nodules	**Channels and voids filled with coarse material; **bioturbation by soil flora
3	240–260	F	F2	Complex; vughy and granular	**Complex packing ***channels ***chambers	11/1	Double spaced porphyric	sa, sr quartz grains (<176 μm ∅)	**	10YR 5/4 yellowish brown, cc fabric	***Nodules	***Nodules	Weakly developed pedality on top of the slide; ****snail shells.
		F	F1	Vughy	***Vughs **channels *chambers	11/1	Double spaced porphyric	sa, sr quartz grains (<250 μm ∅)	**Iron-replaced	10YR 5/4 Yellowish brown, cc fabric	***nodules	***nodules	Weakly developed pedality ****snail shells.
		E		Vughy	****Vughs ***channels **chambers	13/1	Double spaced porphyric	sa, sr quartz grains (<250 μm ∅)	**Iron-replaced	10YR 5/4 yellowish brown, cc fabric	***Nodules	**Nodules	
2	290–310	D	D2	Granular	***Complex packing **channels **chambers ***vesicles	16/1	Open porphyric	sa, sr quartz grains (<250 μm ∅)	**Iron-replaced *$CaCO_3$ replaced	10YR 5/4 yellowish brown, cc fabric	*Nodules *coatings *hypocoatings	***Nodules **coatings **hypocoatings	Less $CaC0_3$ than μfacie D1; * snail shells.
		D	D1	Angular blocky	**Vughs ***channels **chambers ***vesicles *** planes	18/1	Open porphyric	sa, sr quartz grains (<300 μm ∅)	*ch	10YR 5/4 yellowish brown, cc fabric	*Nodules *hypocoatings	****Nodules **coatings, micritic in voids **hypocoatings	Moderated to strongly developed pedality, *snail shells; *complex pedofeatures.
		C	C2	Intergrain pagg regate	*****Complex packing	50/1	Single spaced fine enaulic	sa, sr quartz grains (<353 μm ∅)	–	10YR 5/4 yellowish brown, cc fabric	*Nodules		*Snail shells.
1	310–330	C	C1	Vughy	***Vughs ***complex packing	24/1	Single spaced porphyric	sa, sr quartz grains (<500 μm ∅)	*	10YR 5/4 yellowish brown, cc fabric	*Nodules		****Aggregates from layer B; no snail shells.
		B		Vesicular	***Vughs ***channels ****vesicles	6/1	Fine monic	sa, sr quartz grains (<176 μm ∅)	***Iron-replaced	10YR 5/3 brown, cc fabric	*ty, agg nodules **infillings **coatings **quasicoatings	***Nodules **micritic coatings in voids	Clay and silt microlaminations; channels filled with material from layer C; no snail shells; fauna excrementa.
		A	A1	Vughy	******Vughs **vesicles	8/1	Open porphyric	sa, sr quartz grains (<105 μm ∅)	–	10YR 5/3 brown, cc fabric	**Coatings **hypocoatings	*Nodules	Laminated microstructure the slide, formed by alternated layers of silt; no snail shells.
		A		Vughy	****Vughs **channels **chambers ****vesicles *planes	8/1	Open porphyric	sa, sr quartz grains (<340 μm ∅)	**Iron-replaced	10YR 5/4 yellowish brown, cc fabric	***ty, agg nodules **infillings **hypercoatings **depletion	**Nodules	**Snail shells.

Table 2
AMS dating results.

Lab. Nr.	Depth	Sample type	$^{13}C/^{12}C$ ratio	^{14}C age	1 sigma BP	2 sigmas BP	1 sigma AD	2 sigmas AD	Median BP	Median AD
Beta-310402	360–330 cm	*Olea europaea*	−20.4	1830 ± 30	1732–1814 (1)	1698–1830 (0.963) 1843–1864 (0.036)	136–218 (1)	86–107 (0.036) 120–252 (0.963)	1768	182
Beta-310403	285–260 cm	*Quercus ilex/coccifera*	−24.2	1240 ± 30	1095–1103 (0.044) 1140–1161 (0.173) 1168–1188 (0.200) 1200–1260 (0.581)	1077–1264 (1)	690–750 (0.581) 762–782 (0.200) 789–810 (0.173) 847–855 (0.044)	686–873 (1)	1183	767
Beta-312552	240–220 cm	Unidentified angiosperm	−25.0	1190 ± 30	1068–1143 (0.872) 1159–1169 (0.127)	1006–1029 (0.037) 1053–1180 (0.932) 1209–1230 (0.029)	781–791 (0.127) 807–882 (0.872)	720–741 (0.029) 770–897 (0.932) 921–944 (0.037)	1115	835

complex microstructure (vughy and granular) in the surface horizon (microfacies F2), vughy microstructure in subsurface horizons (microfacies F1) and a moderate organic matter content (0.9%) in relation to the rest of the profile. It is within this layer that the strongest bioturbation of the whole sampled stratigraphic profile is observed in thin section, caused mostly by soil fauna (frequent snail shells, common channels and few biogenic calcium carbonate granules) (Fig. 6, image E; Table 1). Its weakly developed profile, along with the absence of fluvic features such as stratification, decreasing organic carbon content with depth and strong redoximorphic features, points towards the characterisation of this palaeosoil as a Regosol (FAO, 2006).

3.1.7. Layers G, H and I

The dating of layer G (AD 770–944, median AD 835), under which layer F (Regosol) was buried, indicates that this burial event took place in the mid-10th century at the latest. The presence of many channels filled with coarse material and the absence of snail shells indicates that bioturbation in layer G was carried out mostly by soil flora (Fig. 6, image D). Layer G also shows a slight tendency towards an upwards reduction in the percentage of fine and very fine sand grains, and a moderate increase in the proportion of very coarse, coarse and medium silt grains was detected between 242 and 140 cm (layers G, H, I). These data, along with the absence of clear evidences of pedogenesis in thin sections from Kubiena boxes 4 and 5, suggest a continuous and homogenous sedimentation pattern in the context of a moderate and progressive decrease in the energy of the sedimentary agent from the 10th century onwards (Fig. 6, images A–D).

3.2. Source sedimentary materials

All the samples contain the same minerals: quartz (mostly subrounded and subangular polycrystalline) and calcite in higher proportions, and muscovite, illite, dolomite, ankerite, kaolinite, rutile and clinochlore in lesser quantities (Fig. 4).

Geological sources for the torrents that cross Les Arenes are marlstone and calcareous marlstone, formed mainly by calcite and quartz, with lesser quantities of mica, graphite and pyrite. Calcite, quartz and mica in the form of muscovite and illite have been indeed identified through PXRD (Fig. 4). However, the mineralogical homogeneity of the analysed samples prevents the discrimination of different provenances for the sedimentary material. Geoarchaeological data obtained does not allow us to adequately assess the contribution of torrents to the pedosedimentary sequence of Les Arenes either: debris deposited after torrent overflows following torrential rains is formed mostly of coarse-grained organic and inorganic material (Goudie, 2004), and such deposits have not been found in the stratigraphy. PSD analyses show a single mode for every sample in the profile, pointing towards a single agent of transportation and deposition (Fig. 3). Micromorphological features likely to be related to runoff and torrent overflow in Les Arenes, such as depositional surface crusts with abundant vesicles (microfacies A1), could also form in arid and semi-arid regions after flood irrigation or low-energy river floods (Courty et al., 1989; Morin, 1993) (Fig. 5, image D). The most likely scenario so far is that of an uneven alluvial aggradation with minor inputs from seasonal streams to the west of Les Arenes.

3.3. Redoximorphic features

Layer A (380 to 330 cm) is the only one where iron-depleted pedofeatures were identified, along with iron hypocoatings and iron infillings (Fig. 5, images A–C). Iron-depleted pedofeatures are the result of iron dissolution resulting from the prolongation, at least for several months, of water-saturated conditions in the groundmass (Lindbo et al., 2010). On the other hand, both layers A and B show iron/manganese typical aggregate nodules, a redoximorphic feature found in hydromorphic soils (Stoops, 2003) (Fig. 5, image I). Layer B

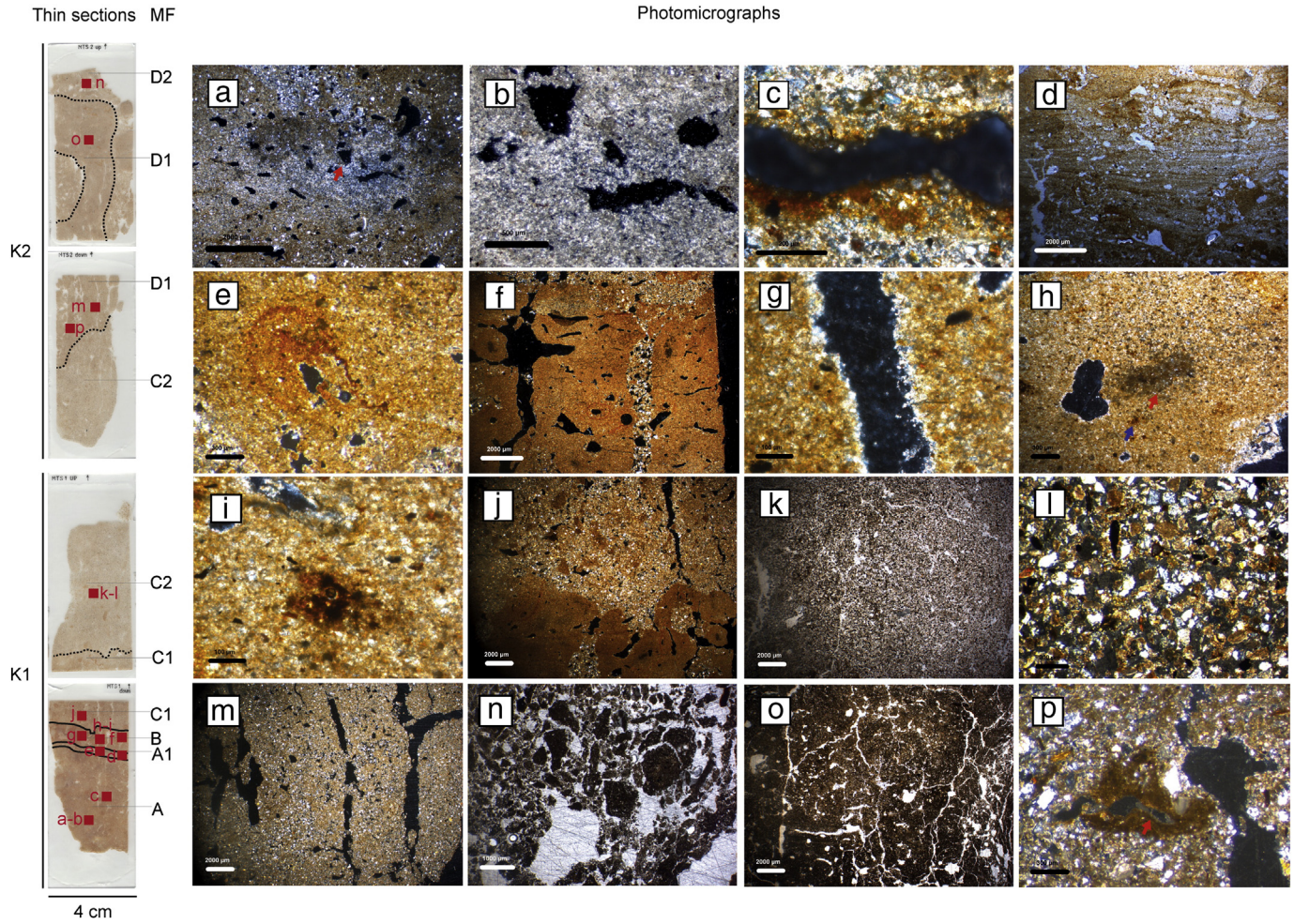

Fig. 5. Correspondence between thin sections from Kubiena (K) boxes 1–2, microfacies (MF) and location of the photomicrographs (red squares), taken under Plane Polarized Light (PPL) and Cross-Polarized Light (XPL). a) Depletion redox pedofeature. Note the white-grey colour in the groundmass caused by iron reduction and subsequent mobilisation. The red arrow shows the detail magnified in image b (XPL). b) Detail of the iron-depleted pedofeature (XPL). c) Iron hypocoating in an iron-depleted groundmass (XPL). d) Microfacies A1 with its submillimetric laminated beds of silt and clayey silt. The presence of vesicles is related to the entrapment of air bubbles when the surface crust dried out. Note the clear boundary between microfacies A1 and layer A underneath (PPL). e) Iron quasicoating coating an iron hypocoating (XPL). f) Channel in layer B filled with coarse material coming down from layer C. Note the parallel and even silty clay laminations in layer B (XPL). g) Micritic coating of a channel in layer B (XPL). h) Orthic calcium carbonate nodule with diffuse boundaries, pointed by a red arrow. The blue arrow indicates the position of the aggregate iron nodule magnified in image i (XPL). i) Aggregate iron nodule (XPL). j) Soil aggregates from layer B incorporated into microfacies C1 due to erosion during deposition of layer C. Note the clear truncation line between layer B and C (XPL). k) Fabric of layer C (PPL). l) Detail of layer C, formed by moderately sorted subrounded and subangular very fine and fine sand grains, mostly polycrystalline quartz (XPL). m) Weakly separated prisms and crystallitic–calcitic b-fabric in the subsurface horizon of the Vertisol (D1). n) Granular microstructure of microfacies D2 (top horizon of the Vertisol) detached from the surface horizon due to shrinking and swelling processes (PPL). o) Angular and subangular wedge-shaped peds in the subsurface horizon of the Vertisol (microfacies D1). Note the planes due to shrinking and swelling and the vesicles and channels caused by bioturbation (PPL). p) Complex textural pedofeature formed by an iron hypocoating coated by a calcium carbonate hypocoating in the subsurface horizon of the Vertisol (microfacies D1). The red arrow indicates the carbonate hypocoating (XPL).

also has few iron quasicoatings, which are usually documented in connection with redox depletion pedofeatures (Driese et al., 1995; McCarthy et al., 1998) (Fig. 5, image E).

Layer C shows few redoximorphic features and very few iron nodules with sharp boundaries. This limited iron content is probably due to the sandy texture and scarcity of organic matter, factors preventing the formation and fixation of Fe and Mn in the groundmass (Fig. 5, images K–L) (Lindbo et al., 2010; Stoops et al., 2010a).

Layer D (Vertisol) has very few iron nodules with sharp boundaries, iron coatings and iron hypocoatings. In general this kind of soils show significant Fe and Mn oxide concentrations (Kovda and Mermut, 2010). The proportion of these redoximorphic features in the Vertisol

Table 3
Mean, median, max, min and range of all physico-chemical analyses.

	Water	Organic	Coal	$CaCO_3$	Mag sus	ARM	HIRM	S_{300}	Grain size
	(%)	(%)	(%)	(%)	(cgs)	(Am^2/kg)			(φ)
Mean	8.817	1.007	0.534	38.402	172.055	2.33×10^{-5}	$6.47 \times 1\,0^{-4}$	0.875	4.539
Median	9.094	1.033	0.543	38.437	171.268	2.35×10^{-5}	$6.22 \times 1\,0^{-4}$	0.870	4.716
Max	13.527	1.454	0.684	42.461	249.753	4.31×10^{-5}	9.11×10^{-4}	0.910	2.539
Min	1.082	0.472	0.374	30.849	98.469	1.08×10^{-5}	$5.07 \times 1\,0^{-4}$	0.847	5.519
Range	12.445	0.982	0.310	11.613	151.284	3.23×10^{-5}	4.04×10^{-4}	0.062	2.980

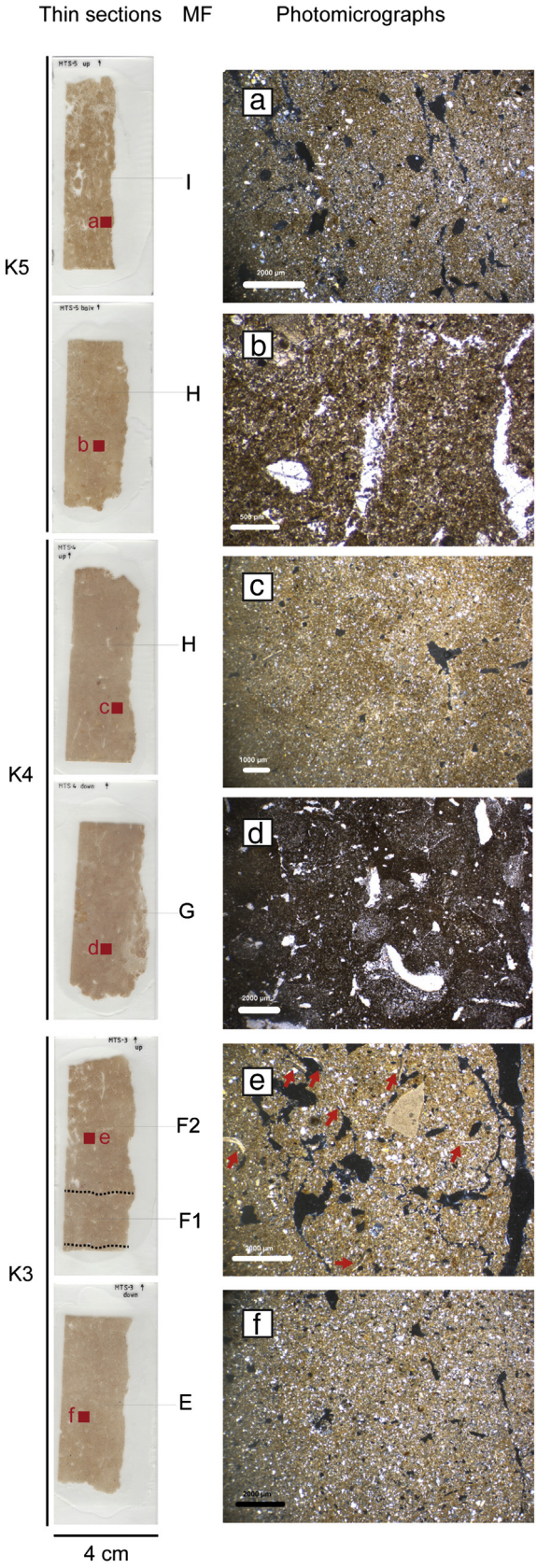

in Les Arenes is thus below normal levels, possibly due to the reduction and subsequent dissolution of iron oxides following prolonged water-saturated conditions. In the next section, the low magnetic values of the Vertisol are shown to be in accord with its characterisation as a soil formed under hydromorphic conditions (De Jong et al., 2000).

In the remaining levels (layers E, G, H, I) few to common iron nodules with sharp and diffuse boundaries, always under 300 μm in diameter, have been found. Their formation suggests water saturation events extending over 2 to 3 days (Lindbo et al., 2010) (Fig. 6, image B).

3.4. Environmental magnetism

Layers A, B and F show peaks of magnetic susceptibility (203.43 cgs; 188.71 cgs and 249.75 cgs respectively) (Fig. 2). Mag Sus values can be affected by magnetite and maghemite contents, because magnetic susceptibility of these ferrimagnetic minerals is 1000 times higher than that of other iron oxides and oxyhydroxides (Mullins, 1977). The correlation coefficient between Mag Sus and ARM averages to $r^2 = 0.44$ when all layers are considered, but it almost doubles to $r^2 = 0.83$ when only layers A, B, C, and D are taken into consideration. This suggests that the magnetic signal at depths 375 to 295 cm is likely to be related to the presence of ferrimagnetic minerals.

Some of the factors involved in the formation of ferrimagnetic minerals such as magnetite and maghemite in soils and sediments are pedogenesis, fire, decomposition of organic matter and succession of wet/dry cycles (Le Borgne, 1955, 1960; Maher, 1986; Maher and Taylor, 1988; Meng et al., 1997; Mullins, 1977; Thompson and Maher, 1995; Tite and Mullins, 1971). The correlation coefficient between ARM and organic matter in Les Arenes is $r^2 = 0.56$ for the whole profile, increasing to $r^2 = 0.65$ when only layers A, B, C and D are taken into consideration. Layers A and B also show higher concentration and diversity of redoximorphic features (Table 1). Frequent alternation between dry and humid conditions results in a greater concentration of ferrimagnetic minerals (Maher and Thompson, 1995). The magnetic signal between 375 and 295 cm seems therefore to be connected with periodical fluctuations in the water content and with the presence of organic matter. The highest concentration of magnetite and maghemite can be found in layers A and B (4.31×10^{-5} and 3.23×10^{-5} respectively) (Table 3), suggesting accentuated reduction–oxidation cycles in these sediments.

The Mag Sus peak detected in layer F (Regosol, 249.75 cgs) (Fig. 2) is not related to the presence of magnetite or maghemite, since ARM values in layer F are negligible. This means that it must be connected to the presence of some mineral with no magnetic remanence. We were not able to identify the provenance of this magnetic signal through PXRD. As shown in Fig. 4, the powder pattern obtained from the Regosol (sample 18) does not show any significant mineralogical difference from the rest. This indicates that the proportion of mineral or minerals that increase the magnetic signal of sample 18 is below detection limit for powder X-ray diffraction (<1%).

The Vertisol (layer D) shows depleted magnetic susceptibility and a low concentration of magnetite and maghemite, as indicated by ARM. Magnetic susceptibility depletion in Vertisols is not uncommon (Tsatskin et al., 2008, 2009). Mediterranean soils developed in aerobic conditions often show enhanced magnetic susceptibility values due to the formation of ferrimagnetic minerals during pedogenesis (Torrent et al., 2010). Those formed in fully hydromorphic

Fig. 6. Correspondence between thin sections from Kubiena (K) boxes 3–5, microfacies (MF) and location of the photomicrographs (red squares), taken under Plane Polarized Light (PPL) and Cross-Polarized Light (XPL). a) Vughy microstructure in a calcitic–crystallitic b-fabric in layer I. Note the absence of pedofeatures (XPL). b) Groundmass of layer H, showing few iron nodules with clear boundaries less than 50 μm in diameter (PPL). c) Vughy microstructure in a calcitic–crystallitic b-fabric in layer H. Note the decrease in fine and very fine sand grains compared to layer F (photomicrograph e) and layer E (photomicrograph f) (XPL). d) Groundmass of layer G, showing channels filled with coarse material and evidences of flora bioturbation (PPL). e) Common snail shells pointed out by red arrows in the top horizon of the highly bioturbated Regosol (layer F) (XPL). f) Groundmass of layer E. Note the abundance of fine and very fine sand grains.

conditions, however, have lower values due to the reduction of Fe and the dissolution of iron oxides (Maher, 1998; Maher and Thompson, 1995). The low concentration of ferrimagnetic minerals and the low quantity of redoximorphic features in the thin sections suggests the prevalence of water-saturated conditions and little alternation between wet and dry cycles in the terrain where the Vertisol was formed.

We used the *L*-Ratio by Liu et al. (2007), which is defined as $IRM_{300\ mT}/IRM_{100\ mT}$, to interpret the HIRM and the *S*-Ratio data. When the *L*-Ratio is stable, variations in HIRM are due to changes in the absolute concentration of haematite and goethite. A variable *L*-Ratio, on the other hand, indicates that changes in HIRM are due to the variation in the coercivity distribution of haematite. In the case of Les Arenes, the correlation between HIRM and the *L*-Ratio indicates that changes in HIRM are indeed caused by fluctuations in the concentration of haematite and goethite (Fig. 7).

The lower absolute concentration of haematite and goethite is found in layers A, B and D (5.14×10^{-4}; 5.12×10^{-4} respectively) (Table 3). The higher concentration, by contrast, is documented in layers F (Regosol) and G (9.11×10^{-4}; 9.01×10^{-4} respectively). In fact, HIRM values increase by 88.16% between layers D and G. In layer H, the absolute concentration of haematite and goethite tends to decrease towards the contacts with layer I (above), where the values become stable. According to Maher et al. (2002) and Maher and Thompson (1995), the persistence of oxidising and dry environmental conditions promotes the formation of haematite and goethite, the more oxic forms of iron. Regarding the *S*-$Ratio_{300}$, all values are between 0.91 and 0.85, indicating that, despite the fluctuations, the magnetic component is basically dominated by magnetite and/or maghemite (Dalan and Banerjee, 1998).

3.5. Socio-ecological dynamics (layers A–I)

Overall, data gathered from the sedimentary sequence of Les Arenes clarify the evolution of the floodplain in terms of its hydrological regime and fluctuations between wet and dry conditions during the 1st millennium AD. Predominance of wet conditions, long periods of soil formation and uncommon high-intensity floods seem to have been the main features of the wetland between AD 86 and 686. Drier conditions and an increase in the frequency and intensity of flooding are documented starting from AD 686 to 873 (median AD 767), overlapping with the onset of the Andalusi period (AD 711). After a short period of pedogenesis coinciding with the longest dry period of the 1st millennium AD, continuous floods of moderate intensity are attested between AD 720 and 944 (median AD 835).

3.5.1. The climatic factor

Physico-chemical analysis and soil micromorphology for layers A–D point towards seasonal fluctuations in soil/sediment moisture in the context of a generally low to medium-energy wet depositional environment between the 1st and the 7th centuries AD. Ferrimagnetic minerals, redoximorphic features and carbonate precipitation in the form of irregular calcium carbonate orthic nodules with diffuse boundaries are likely to be related to wetting and drying processes typical of active Mediterranean wetlands. Predominance of low to medium-energy floods is suggested by the combined occurrence of medium particle size average (4.5 φ, coarse silt), microlaminated deposits of silt and silty clay and two different cycles of pedogenesis (Fluvisol and Vertisol). Floodplain geomorphology and the presence of a relict point bar deposit 320–300 cm below the current surface (layer C) suggest that the area selected for sampling was located very close to the river shore between AD 86 and 686, thus being strongly affected by the hydrological fluctuations of the Ebro River. Seasonal flooding of the alluvial plain seems to have been responsible for the periodical waterlogging of soils in the sampling area before the 7th century AD. The predominance of humid conditions between the 1st and 7th centuries AD is indicated by redoximorphic features related with hydromorphism (iron-depleted pedofeatures, typical aggregate iron nodules, iron coatings and hypocoatings); by higher organic matter content in relation to the rest of the stratigraphic profile; and by the presence of a magnetically depleted Vertisol 300–290 cm under the current surface.

The predominance of wet environmental conditions in Les Arenes between the 1st and 7th centuries AD overlaps with two major humid climatic trends: the end of the Iberian-Roman Humid Period (IRHP, c. 650 BC–AD 450) and the Dark Ages Humid Period (DAHP, c. AD 500–800), both likely caused by a negative shift in the North Atlantic Oscillation (NAO) and a decline in solar output (Cacho et al., 2010; Cheyette, 2008; Martin-Puertas et al., 2008, 2009). AD 150–350 seems to have been the wettest period of the last 2500 years in the Iberian Peninsula (Cacho et al., 2010). Features detected in layer A (AD 86–252, median AD 182), such as iron-depletion, aggregate iron nodules, laminated beds and an upwards decrease in the content of sand grains, agree with the predominance of strong wet conditions in a depositional environment characterised by decreasing energy and low peak discharges. The occurrence of reduced river activity and humid conditions during the late Roman period has also been attested in France, in the Upper and Middle Rhône (AD 100–300; Arnaud et al., 2005; Provansal et al., 1999); in Tunis, in the Medjerda alluvial basin (<AD 250; Faust et al., 2004); and in Italy, in the stretch of the river Tiber throughout Rome, which was flooded fewer times between AD 200–500 (Giraudi, 2005). The incipient development of a Fluvisol confirms in Les Arenes the trend towards a lower hydrological regime by the end of the 3rd century AD. Although layer C (AD 252–686) can be related to a high-magnitude flood, overall data indicate that extreme events were highly exceptional during the first half of the 1st millennium AD. A very different environment in the same period was that of the coastal floodplain of the Arno River, in Italy, whose channel changed its course several times before AD 500 due to the concurrent effects of sea-level rise and high-magnitude flood events (Benvenuti et al., 2006).

An increase in the frequency and intensity of flooding is documented in Spain, Great Britain and Poland in AD 570, 660 and 860–865 (Macklin et al., 2006). Strong humid conditions in France are attested between AD 664 and 887 in the lower Doubs Valley (Vannière et al., 2003) and in the Rhône Valley, where torrential rains led to a rise in the water table causing waterlogging of the fields between AD 500 and 800 (Arnaud et al., 2005; Provansal et al., 1999; Verdin et al., 2001). In central Turkey, palaeoenvironmental data recovered from Tecer Lake point towards

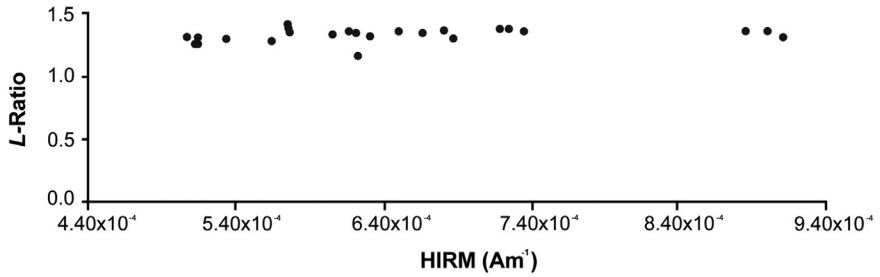

Fig. 7. Dispersion graph showing *L*-Ratio against HIRM values.

a significant decrease in evaporation and predominance of humid conditions for the same period (Kuzucuoglu et al., 2011). In central Italy, the 6th–9th centuries were a period characterised by a cooler, wetter climate and increasing flooding (Giraudi, 2005). Colder environmental conditions have also been detected in central Europe: Holzhauser et al. (2005) documented an increase in ice masses in the Alps between AD 500 and 600 and AD 800 and 900, while Barber et al. (2004) found that bogs in northern Germany and Denmark expanded around AD 550. In that sense, the 6th century seems to mark a shift from a low hydrological regime to an enhanced activity of Mediterranean rivers caused partially by a climatic change (Fig. 8), leading to a cooling of the environment and higher precipitations. Wet conditions during the DAHP are clearly attested in Les Arenes by the hydromorphic Vertisol, formed before AD 686–873. However, pedogenesis during that period indicates that Les Arenes was then a relatively stable floodplain with minor alluvial aggradation and long periods of soil formation. An increase in the frequency and intensity of floods appear to happen only between AD 686 and 873 (median AD 767), according to the higher proportion of fine and very fine sand grains in layer E and the lack of evidences of pedogenesis. The onset of floods with higher frequency and intensity is also documented for that period (AD 785) in the Tagus River, C Spain (Benito et al., 2003).

Enhanced river activity starting from AD 686 to 873 concurs in Les Arenes with a shift towards drier environmental conditions. Less quantity and variety of redoximorphic features in thin section from layer E upwards indicate a significant decrease both in the frequency and duration of water saturated conditions, extending over few days at the most. This coincides with the 88% increase in the absolute concentration of haematite and goethite detected between layers E and

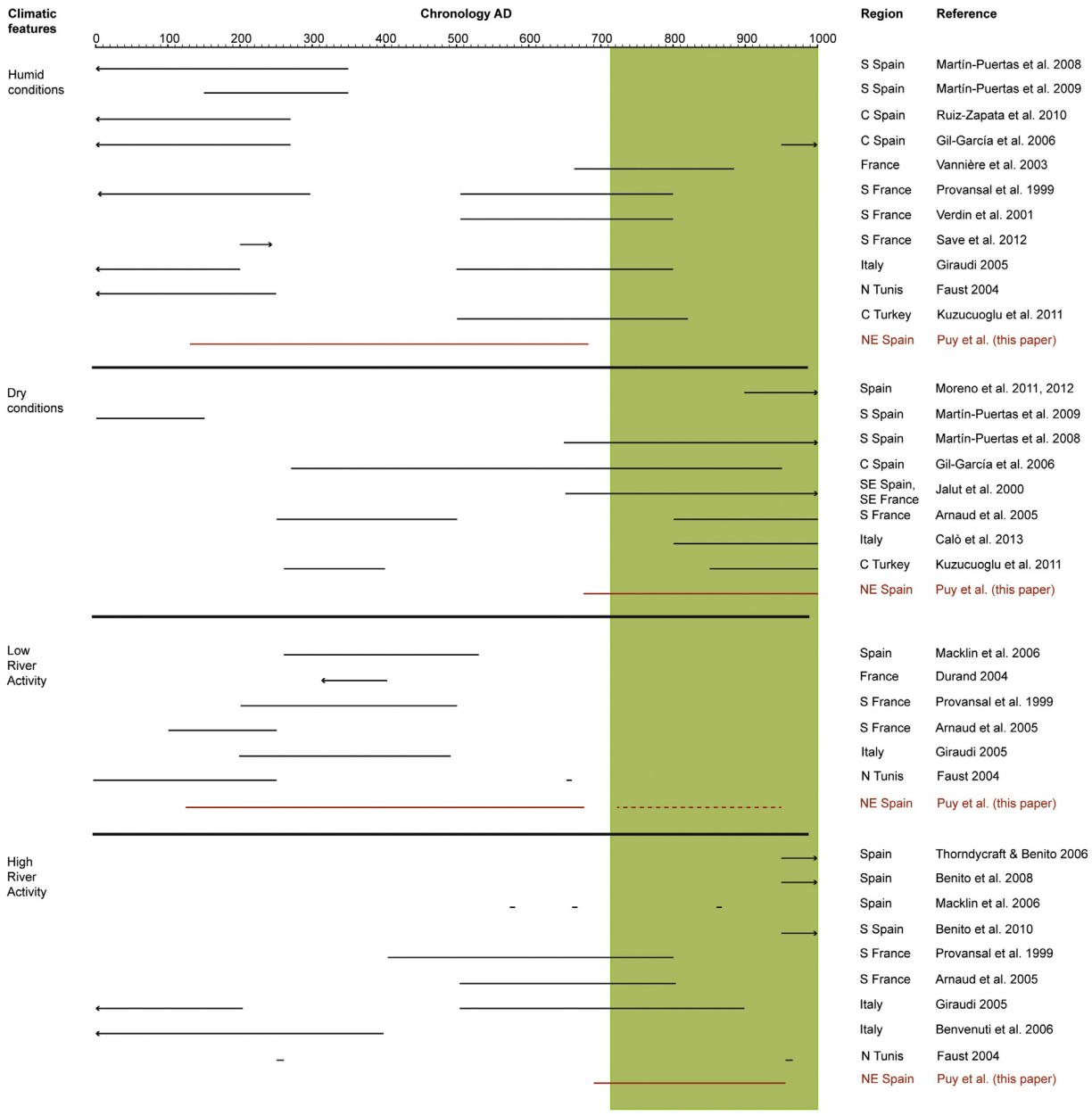

Fig. 8. Graph showing the predominance of humid/dry conditions and low/high river activity in different Mediterranean settings during the 1st millennium AD after the references mentioned in the paper. Data obtained from Les Arenes appears in red after the reference Puy et al. (this paper). The red-dotted line refers to the longest possible period of soil stability that existed before the burial of the Regosol, according to the AMS dates (AD 720–944). The green colour encompasses the al-Andalus period, starting in AD 711.

G. The formation of goethite is favoured by high oxidation rates and formation of haematite by high temperatures and decreased water activity; therefore, an increase in the concentration of both antiferromagnetic minerals indicates longer periods of dryness (Maher et al., 2002; Schwertmann, 1988; Taylor et al., 1987). Higher dryness and higher flooding activity has been also documented in several Spanish and European fluvial systems during the Medieval Climate Anomaly (MCA c. AD 900–1200; Benito et al., 2008, 2010; Machado et al., 2011; Thorndycraft and Benito, 2006; Wilhelm et al., 2013), although lake and marine sediments from NE Spain seem to point towards a lower hydrological regime for the same period (Moreno et al., 2011, 2012).

The shift towards a warmer climate during the MCA has been attested in many different environments of the Iberian Peninsula and beyond, apart from floodplains and river systems: e.g. caves in Cantabria (N Spain) (Martín-Chivelet et al., 2011); lakes in Pyrenees (NE Spain) (Morellón et al., 2009), Córdoba (S Spain) (Martin-Puertas et al., 2008), Pantelleria Island (between Sicily and Tunis) (Calò et al., 2013) or the Sivas basin (Central Turkey) (Kuzucuoglu et al., 2011); and in wetlands in La Mancha (Central Spain) (Gil García et al., 2006). It seems to have been a global phenomenon (Mann et al., 2009), despite significant heterogeneities both in space and time. Drier conditions during the MCA were likely caused by an increase in the solar radiation and NAO, resulting in a warmer and arid climate in the Mediterranean region (Moreno et al., 2012). Dry conditions seem to have fully predominated in Les Arenes at some point between AD 686 and 873/720 and 944, when the Regosol (layer F) was formed. The highest absolute concentration of antiferromagnetic minerals on the whole stratigraphic profile is found in the Regosol (9.11×10^{-4}), suggesting that pedogenesis took place during the longest dry period of the 1st millennium AD. Soil formation process, along with few redoximorphic features in thin sections and a decrease in the content of sand grains, points towards lower hydrological activity and almost no alternation between wet and dry conditions for that period.

Finally, after slight increases in the content of fine and very fine sand grains in layers G and H, the absence of pedofeatures in thin sections and the progressive decrease in the percentage of the coarse fraction suggest continuous floods of lower energy after the second half of the 10th century AD.

3.5.2. The anthropic factor

The onset of drier climatic conditions in Les Arenes overlaps with the Andalusi period (AD 711–1148), when Arabic-Berber tribes and clans entered the Iberian Peninsula (al-Andalus). Irrigated agriculture became the main agrarian strategy of peasant communities and a wide range of Asian crops, such as the orange and lemon trees, the aubergine, the cucumber and the colocasia, were introduced for the first time in the Western Mediterranean (Barceló, 1986; Glick and Kirchner, 2000; Watson, 1983). New agrarian landscapes were implemented following the Arab-Berber migration and settlement, and several hydraulic systems were constructed to claim agricultural lands in terrains as different as alluvial plains, valley slopes, ravines or hills (Barceló and Retamero, 2005; Guinot, 2005; Kirchner, 1997). Wetlands and floodable areas seem to have been generally rejected for intensive cropping due to their seasonal fluctuations and dynamism, which jeopardised the stability and structured growing strategies required for traditional irrigated agriculture (Puy, 2014). However, far from being overlooked by the newly arrived communities, wetlands seem to have been used in Andalusi times for fishing, hunting, gathering and cattle grazing, as seen in the ravines of Menorca (Balearic Islands) and in marshes of the Lower Segura River (Alicante) (Azuar and Gutiérrez, 1999; Barceló and Retamero, 2005). The floodplains of the middle Segura Basin (Murcia) were cropped only after the retreat of the waterline (Puy, 2012, 2014). Wetlands on the Eastern coast of the Iberian Peninsula, which were partially drained after the feudal conquest of the 13th century AD, seem to have been rejected for irrigated agriculture during the Andalusi period (Torró, 2010). Although no absolute dates were obtained, the coastal wetland of Pla de la Vila (Ibiza, Balearic Islands) stands to date as the only humid area that could have been partially drained during Andalusi times (AD 902–1235) (Barceló et al., 1997).

The shift towards drier conditions detected in the stratigraphic profile of Les Arenes between the 7th and 9th centuries AD broadly concurs with the MCA, and no direct evidence to date allows relating this trend to desiccation through drainage. However, we think that anthropic influence has to be also taken into account for the following reasons:

1. Different sets of processes can result in the same features due to equifinality, which is a major concern for researchers focused on weighing the role of social and ecological factors in the shaping of the environment (Walkington, 2010). Higher oxidation, less wetting and drying cycles and terrain consolidation are consequences to be expected in the soil following the onset of drier climatic conditions but may also result from artificial drainage.
2. Research on Andalusi agrarian areas has shown that the texts written shortly after the feudal conquest of the 11th–15th centuries AD provide valuable information regarding pre-existing Andalusi fields (Barceló and Retamero, 2005; Barceló et al., 1998; Kirchner, 1997, 2002; Sitjes, 2010; Virgili, 2010). Circa sixty-four texts written between AD 1148 and 1210 mention the name of Andalusi tenants, canals and plots in Les Arenes. The study of the texts revealed an orthogonal network of canals, the major ones bordering the plots in the E and W sides, and the minor ones in the N and S sides (Virgili, 2010). The considerable amount of historical records referring to canals, plots and Andalusi farmers immediately after AD 1148 suggests that the initial orthogonal drainage network was already in place and fully operative when the feudal lords arrived. This does not exclude that further development of the same network may have been put in place by the feudal lords to reclaim more land and increase revenues.
3. Work carried out over the last 30 years in the Balearic Islands (Barceló, 2001; Barceló and Retamero, 2005; Kirchner, 1997, 2009), S and SE Spain (Barceló et al., 1998; Navarro, 1995; Puy, 2012, 2014; Puy and Balbo, 2013), and E Spain (Esquilache, 2011; Guinot and Esquilache, 2012; Torró, 2007; Vea, 1996) suggested Arab-Berber groups changed the previous landscape and constructed their cropping fields immediately after settling in these regions. Furthermore, work by Puy and Balbo (2013) in the Andalusi irrigated fields of Ricote (Murcia, SE Spain) allowed to obtain an absolute date of AD 647–778 (median AD 706) for the first construction of the Ricote agrarian area, which implied a swift transformation of a slightly saline hypercalcic Calcisol into a highly productive irrigated field. The date obtained for the onset of drier conditions in Les Arenes is AD 686–873 (median AD 767); Arab-Berber groups are attested in Tortosa from the 8th century AD onwards (Barceló, 1999; Barceló and Kirchner, 1992) and drainage canals are mentioned in records from the 12th century AD (Virgili, 2010). Andalusi groups may therefore have contributed to the drying of Les Arenes by implementing a network of drainage canals shortly after AD 711, thus reinforcing the effects of on-going regional climatic trends leading to the extension of dry land in Les Arenes floodplain.

Further excavation and dating of drainage canals, sediment infillings and marshland sedimentary sequences will allow a precise assessment of the role played by Arab-Berber groups in the first stages of wetland reclamation for agriculture in al-Andalus. This integrated methodological framework has been effectively applied to obtain valuable information regarding the pace of the drainage and the interactions between past populations and the environment in the marshy areas of the Rhône Valley, in France (Bernigaud et al., 2011; Delhon et al., 2013; Verdin et al., 2001).

Although several researchers agreed in characterising al-Andalus as a period of profound environmental transformations (Glick, 1991), socio-ecological analyses aimed at disentangling the interplay between

Arab-Berbers, ecology and climate have been extremely rare (Puy and Balbo, 2013). More information is needed on the pre-existent environments, the adaptive responses of these groups to climatic trends and the scope of the edaphological changes brought about by the construction of their cropping fields. In our case, the interplay between the onset of drier climatic conditions and the settling of Arab-Berbers in Tortosa likely generated a reinforcing feedback loop, accelerating the on-going desiccation of a former wet floodplain through the construction of the first drainage canals. Extension of research to western portions of Les Arenes and to similar contexts in the Iberian Peninsula will improve our perception of the dynamics between environment, climate and Andalusi groups, and their intertwined role in the formation of our current Mediterranean landscapes.

4. Conclusions

The integration of historical records and geoarchaeological data collected from a sedimentary sequence in Les Arenes (Tortosa, NE Spain) allowed understanding the socio-ecological dynamics of a typical Mediterranean floodplain during the 1st millennium AD. Predominance of humid conditions and a low to medium-energy depositional environment characterised Les Arenes between the 1st and the 7th century AD, broadly coinciding with the Iberian Roman Humid Period (IRHP, c. 650 BC–AD 450) and the Dark Age Humid Period (DAHP, c. AD 500–800). Onset of drier conditions and enhanced river activity are documented starting from AD 686, followed by a lower hydrological regime and the longest dry period of the 1st millennium at some point between AD 686 and 873/720 and 944. The shift towards dry conditions in Les Arenes overlaps with the Medieval Climate Anomaly (MCA, c. 900–1200) and the al-Andalus period (AD 711–1148), characterised by the arrival of several Arab-Berber groups to the Iberian Peninsula, including Tortosa. Since Les Arenes appears partially drained in written records issued shortly after the feudal conquest of Tortosa (AD 1148), which led to the extinction of the pre-existent Andalusi population, it seems likely that Andalusi groups contributed to the on-going desiccation of the floodplain by means of drainage. Our results stress the need to integrate written records and geoarchaeological datasets in order to adequately assess the socio-ecological dynamics of Mediterranean wetlands during the last 2000 years. Moreover, we highlight the need to combine climatic and anthropic factors when studying the scope of the environmental changes brought about in the Iberian Peninsula by Andalusi groups after AD 711.

Acknowledgements

Joan Martínez Tomàs (Servei d'Arqueologia i Paleontologia, Departament de Cultura i Mitjans de Comunicació, Generalitat de Catalunya) provided critical support during fieldwork. Josep Marfull and María Lorente (UAB) participated in the sampling of the profile in Les Arenes, Tortosa. For their help and suggestions we would also like to thank Dr Itxaso Sopelana (ICAC); Elisabet Beamud, from Laboratori de Paleomagnetisme (CCITUB-ICTJA CSIC); Montserrat Guart, from the Departament d'Estratigrafía, Paleontologia i Geociències Marines, Universitat de Barcelona (UB); Dr Ángel Álvarez and Javier Martínez, from the Servei de Difracció de Raigs X, Universitat Autònoma de Barcelona (UAB); Asier Santana, from Micromorfología de sòls i anàlisi d'imatges, Universitat de Lleida (UL); and Prof Marco Madella, Department of Archaeology and Anthropology, Institució Milà i Fontanals, Spanish National Research Council (CSIC). We are also grateful to the Editor of Geoderma and two anonymous reviewers who made valuable comments on an earlier version of this paper. All mistakes and shortcomings remain our own. Arnald Puy received the support of the Spanish Ministry of Science and Innovation through a FPI fellowship (BES-2008-002037) linked to the projects 'Acclimatization and diffusion of plants in al-Andalus' (HUM 2007-62899/HIST) and 'Choices and plant management in al-Andalus. Peasant practices and states' (HAR2010-21932). Andrea Balbo has worked on this paper on contracts from SimulPast Consolider CSD2010-00034 and Juan de la Cierva Programme (JCI-2011-10734). Antoni Virgili is a member of the research team of the projects 'Acclimatization and diffusion of plants in al-Andalus' (HUM 2007-62899/HIST) and 'Choices and plant management in al-Andalus. Peasant practices and states' (HAR2010-21932). The research was carried out within the framework of the projects 'Rural settlements in the lower Ebre and the City of Tortosa (Catalonia, Spain) before and after the feudal conquest (11–12th centuries)', funded by the Departament de Cultura i Mitjans de Comunicació of the Generalitat de Catalunya (Government of Catalonia) (511K121 2012NP43/8430), PIs Dr Helena Kirchner and Antoni Virgili; 'Acclimatization and diffusion of plants in al-Andalus' (HUM 2007-62899/HIST), PI Helena Kirchner, and 'Choices and plant management in al-Andalus. Peasant practices and states' (HAR2010-21932), PI Helena Kirchner; both funded by the Ministerio de Ciencia e Innovación, Spanish Government.

Appendix A. Supplementary data

Supplementary data associated with this article can be found in the online version, at http://dx.doi.org/10.1016/j.geoderma.2014.05.001. These data include Google maps of the most important areas described in this article.

References

Agenda 21 local de Tortosa, 2009. Memòria.
Amorosi, A., Bini, M., Giacomelli, S., Pappalardo, M., Ribecai, C., Rossi, V., Sammartino, I., Sarti, G., 2013. Middle to late Holocene environmental evolution of the Pisa coastal plain (Tuscany, Italy) and early human settlements. Quat. Int. 303, 93–106.
Anuario de Aforos, 2010. Minist. Agric. Aliment. y Medio Ambient. URL http://sig.magrama.es/93/ClienteWS/GISROEA/default.aspx?nombre=ROAN_ESTACION_AFORO_RIOS&claves=COD_HIDRO%7COD_SITUACION_ESTACION&valores=9027%7C4 (Accessed 16 February 2014).
Arasa Tuliesa, A., 1994. Depósitos cuaternarios en el Bajo Ebro: características estratigráficas y deposicionales. Geogaceta 15, 98–101.
Arnaud, F., Revel, M., Chapron, E., Desmet, M., Tribovillard, N., 2005. 7200 years of Rhône river flooding activity in Lake Le Bourget, France: a high-resolution sediment record of NW Alps hydrology. The Holocene 15, 420–428.
Azuar, R., Gutiérrez, S., 1999. Formación y transformación de un espaico agrícola islámico en el sur del País Valenciano: el Bajo Segura (siglos IX–XIII). In: Bazzana, A. (Ed.), Castrum 5. Archéologie des Espaces Agraires Mediterranées au Moyen Âge. Casa de Velázquez, Madrid, pp. 201–211.
Balbo, A.L., 2008. Human Adaptation to Mediterranean Wetlands: The Geoarchaeology of Polje Čepić (Istria, Croatia) in the Late Pleistocene and Holocene, VDM Verlag Dr. Müller, Germany.
Balbo, A.L., Andrič, M., Rubinić, J., Moscariello, A., Miracle, P.T., 2006. Palaeoenvironmental and archaeological implications of a sediment core from Polje Čepić, Istria, Croatia. Geol. Croat. 59, 109–124.
Barber, K., Chambers, F., Maddy, D., 2004. Late Holocene climatic history of northern Germany and Denmark: peat macrofossil investigations at Dosenmoor, Schleswig-Holstein, and Svanemose, Jutland. Boreas 33, 132–144.
Barceló, M., 1986. La qüestió de l'hidraulisme andalusí. In: Barceló, M., Carbonero, M.A., Martí, R., Rosselló-Bordoy, G. (Eds.), Les Aigües Cercades. Els Qanat(s) de L'illa de Mallorca. Institut d'Estudis Baleàrics, Palma de Mallorca, pp. 9–36.
Barceló, M. (Ed.), 1999. Musulmans i Catalunya. Empúries, Barcelona.
Barceló, M., 2001. Immigration berbère et établissements paysand dans l'île d'Eivissa, 902–1235: à la recherche de la logique de la construccion d'une nouvelle société. In: Martin, J.M. (Ed.), Castrum VII. Zones Côtières et Plaines Littorales dans le Monde Méditerranée au Moyen Âge: Défense, Peuplement, Mise en Valeur. Casa de Velázquez, Madrid, pp. 291–321.
Barceló, M., Kirchner, H., 1992. Husun et établissements arabo-berbères de la Frontière Supérieure (zone de l'actuelle Catalogne) d'Al-Andalus. In: Poisson, J.M. (Ed.), Castrum 4.Frontière et Peuplement dans le Monde Méditerranéen au Moyen Age. Casa de Velázquez, Madrid, pp. 61–73.
Barceló, M., Retamero, F., 2005. Els Barrancs Tancats. L'Ordre Pagès al Sud de Menorca en Època Andalusina, Institut Menorquí d'Estudis, Menorca.
Barceló, M., Kirchner, H., Navarro, C., 1995. El Agua que no Duerme. Fundamentos de la Arqueología Hidráulica Andalusí, Granada, El Legado Andalusí.
Barceló, M., González Villaescusa, R., Kirchner, H., 1997. La construction d'un espace agraire drainé au awz de la Madīna de Yābisa (Ibiza, Baléares), In: Burnouf, J., Bravard, J.P., Chouquer, G. (Eds.), La Dynamique des Paysages Protohistoriques, Antiques, Médiévaux et Modernes. Actes des Recontres Internationales d'Archéologie et d'Histoire d'Antibes, Éditions APDCA., pp. 113–125 (Sophia Antipolis).
Barceló, M., Kirchner, H., Martí, R., Torres, J.M., 1998. The design of irrigation systems in al-Andalus. The Cases of Guajar Faragüit (Los Guájares, Granada, Spain) and Castellitx,

Aubenya and Biniatró (Balearic Islands), Universitat Autònoma de Barcelona, Bellaterra.
Batalla, R.J., Gómez, C.M., Kondolf, G.M.M., Gomez, C.M., 2004. Reservoir-induced hydrological changes in the Ebro River basin (NE Spain). J. Hydrol. 290, 117–136.
Batalla, R.J., Vericat, D., Palau, A., 2008. Efectos de las presas en la dinámica geomorfológica del tramo bajo del Ebro. Crecidas controladas. Ing. del agua 15, 243–255.
Benito, G., Sopeña, A., Sánchez-Moya, Y., Machado, M.J., Pérez-González, A., 2003. Palaeoflood record of the Tagus River (Central Spain) during the Late Pleistocene and Holocene. Quat. Sci. Rev. 22, 1737–1756.
Benito, G., Thorndycraft, V., Rico, M., 2008. Palaeoflood and floodplain records from Spain: evidence for long-term climate variability and environmental changes. Geomorphology 101, 68–77.
Benito, G., Rico, M., Sánchez-Moya, Y., Sopeña, A., Thorndycraft, V.R., 2010. The impact of late Holocene climatic variability and land use change on the flood hydrology of the Guadalentín River, southeast Spain. Glob. Planet. Chang. 70, 53–63.
Benvenuti, M., Mariotti-Lippi, M., Pallecchi, P., Sagri, M., 2006. Late-Holocene catastrophic floods in the terminal Arno River (Pisa, Central Italy) from the story of a Roman riverine harbour. The Holocene 16, 863–876.
Benyarku, C.A., Stoops, G., 2005. Guidelines for Preparation of Rock and Soil Thin Sections and Polished Sections, Laboratorium Voor Mineralogie, Petrologie and Micropedologie, Belgium.
Bernigaud, N., Berger, J.F., Bleu, S., Bouby, L., Delhon, C., Franc, O., Gaucher, G., Latour-Argant, C., 2011. La bonification antique des grands marais de Bourgoin-La Verpillière (Isère): colonisation, grande hydraulique agricole et mise en culture pendant le Haut-Empire. In: Mathieu, N., Rémy, B., Leveau, P. (Eds.), L'Eau dans les Alpes Occidentales à l'Époque Romaine. Cahier du CRHIPA, 19, pp. 265–289.
Bramon, D., 2002. De Quan Érem o no Érem Musulmans. Textos del 713 al 10102nd ed., Eumo, Vic.
Bresson, L., Valentin, C., 1993. Soil surface crust formation: contribution of micromorphology. Soil Micromorphol. Stud. Manag. Genesis. Proc. IX Int. Work. Meet. Soil Micromorphol., 22, pp. 737–762.
Broothaerts, N., Verstraeten, G., Notebaert, B., Assendelft, R., Kasse, C., Bohncke, S., Vandenberghe, J., 2013. Sensitivity of floodplain geoecology to human impact: a Holocene perspective for the headwaters of the Dijile catchment, central Belgium. The Holocene 23, 1403–1414.
Budja, M., Mlekuz, D., 2010. Lake or floodplain? Mid-Holocene settlement patterns and the landscape dynamic of the Izica floodplain (Ljubljana Marshes, Slovenia). The Holocene 20, 1269–1275.
Cacho, I., Valero Garcés, B., González Sampériz, P., 2010. Revisión de las reconstrucciones paleoclimáticas en la Península Ibérica desde el último periodo glacial. In: Pérez, F.F., Boscolo, R. (Eds.), Clima en España: Pasado, Presente y Futuro. MARM-MICINN, Madrid, pp. 9–24.
Calò, C., Henne, P.D., Eugster, P., van Leeuwen, J., Gilli, A., Hamann, Y., La Mantia, T., Pasta, S., Vescovi, E., Tinner, W., 2013. 1200 years of decadal-scale variability of Mediterranean vegetation and climate at Pantelleria Island, Italy. The Holocene 23, 1477–1486.
Cheyette, F.L., 2008. The disappearance of the ancient landscape and the climatic anomaly of the early Middle Ages: a question to be pursued. Early Mediev. Eur. 16, 127–165.
Courty, M.A., Goldberg, P., Macphail, R.I., 1989. Soils and Micromorphology in Archaeology, Cambridge University Press, Cambridge.
Dalan, R.A., Banerjee, S.K., 1998. Solving archaeological problems using techniques of soil magnetism. Geoarchaeol 13, 3–36.
Daoud-Bouattour, A., Muller, S.D., Jamaa, H.F.-B., Saad-Limam, S. Ben, Rhazi, L., Soulié-Märsche, I., Rouissi, M., Touati, B., Jilani, I.B.H., Gammar, A.M., Ghrabi-Gammar, Z., 2011. Conservation of Mediterranean wetlands: interest of historical approach. C. R. Biol. 334, 742–756.
De Jong, E., Pennock, D., Nestor, P., 2000. Magnetic susceptibility of soils in different slope positions in Saskatchewan, Canada. Catena 40, 291–305.
Delhon, C., Bernigaud, N., Berger, J.F., Salvador, P.G., Thiébault, S., Ploton, M., 2013. Evolution and management of humid landscapes in northern Dauphiné (Rhone valley, France): contribution of charcoal and wood studies. The Holocene 23, 1447–1465.
Dorado Valiño, M., Valdeolmillos Rodríguez, A., Blanca Ruiz Zapata, M., José Gil García, M., de Bustamante Gutiérrez, I., 2002. Climatic changes since the Late-glacial/Holocene transition in La Mancha Plain (South-central Iberian Peninsula, Spain) and their incidence on Las Tablas de Daimiel marshlands. Quat. Int. 93–94, 73–84.
Driese, S.G., Simpson, E.L., Eriksson, K.A., 1995. Redoximorohic paleosols in alluvial and lacustrine deposits, 1.8 Ga Lochness Formation, Mount Isa, Australia: pedogenic processes and implications for paleoclimate. J. Sediment. Res. 65, 675–689.
Durand, N., Curtis Monger, H., Canti, M.G., 2010. Calcium carbonate features. Interpretation of Micromorphological Features of Soils and Regoliths. Elsevier, Oxford, pp. 149–194.
Esquilache, F., 2011. L'evolució del paisatge agrari andalusí i feudal de les grans hortes fluvials. Les sèquies de Quart i del Comuner d'Aldaia a l'horta de València. Recerques, 62, pp. 5–36.
Evans, M.E., Heller, F., 1991. Environmental Magnetism. Principles and Applications of Enviromagnetics, Elsevier, California.
FAO, 2006. World Reference Base for Soil Resources. A Framework for International Classification, Correlation and Communication, Publishing Management Service.
Faust, D., Zielhofer, C., Baena Escudero, R., Díaz del Olmo, F., 2004. High-resolution fluvial record of late Holocene geomorphic change in northern Tunisia: climatic or human impact? Quat. Sci. Rev. 23, 1757–1775.
Folk, R.L., Ward, W.C., 1957. Brazos River bar: a study in the significance of grain size parameters. J. Sediment. Petrol. 27, 3–26.
Friedman, G.M., Sanders, J.E., 1978. Principles of Sedimentology, Wiley, New York.
Gil García, M.J., Ruiz Zapata, M.B., Santisteban, J.I., Mediavilla, R., López-Pamo, E., Dabrio, C.J., 2006. Late Holocene environments in Las Tablas de Daimiel (south central Iberian Peninsula, Spain). Veg. Hist. Archaeobot. 16, 241–250.
Giraudi, C., 2005. Late-Holocene alluvial events in the Central Apennines, Italy. The Holocene 15, 768–773.
Giraudi, C., Magny, M., Zanchetta, G., Drysdale, R.N., 2011. The Holocene climatic evolution of Mediterranean Italy: a review of the continental geological data. The Holocene 21, 105–115.
Glick, T.F., 1991. Cristianos y Musulmanes en la España Medieval, Alianza Editorial, Madrid pp. 711–1250.
Glick, T.F., Kirchner, H., 2000. Hydraulic systems and technologies of Islamic Spain: history and archaeology. In: Squatriti, P. (Ed.), Working with Water in Medieval Europe: Technology and Resource-use. Brill, Leiden-Boston-Köln, pp. 267–329.
Goudie, A.S. (Ed.), 2004. Encyclopedia of Geomorphology. Routledge, London, New York.
Guido, M.A., Menozzi, B.I., Bellini, C., Placereani, S., Montanari, C., 2013. A palynological contribution to the environmental archaeology of a Mediterranean mountain wetland (North West Apennines, Italy). The Holocene 23, 1517–1527.
Guinot, E., 2005. L'horta de València a la baixa Edat Mitjana. De sistema hidràulic andalusí a feudal. Afers, 51, pp. 271–300.
Guinot, E., Esquilache, F., 2012. La reorganización del paisaje agrario en la huerta de Valencia después de la conquista cristiana. El sistema hidráulico y el parcelario de Montcada y Benifaraig en el siglo XIII. Debates Arqueol. Mediev., 2, pp. 229–276.
Gurnell, A.M., Petts, G.E., 2002. Island-dominated landscapes of large floodplain rivers, a European perspective. Freshw. Biol. 47, 581–600.
Heiri, O., Lotter, A., Lemcke, G., 2001. Loss on ignition as a method for estimating organic and carbonate content in sediments: reproducibility and comparability of results. J. Paleolimnol. 25, 101–110.
Hodgson, J.M., 1976. Soil survey field handbook. Technical Monograph 5. Soil Survey, Harpenden.
Holzhauser, H., Magny, M.J., Zumbühl, H.J., 2005. Glacier and lake-level variations in west-central Europe over the last 3500 years. The Holocene 15, 789–801.
Horden, P., Purcell, N., 2000. The Corrupting Sea. A Study of Mediterranean History, Blackwell Publishing, London.
Ibáñez, C., Prat, N., 2003. The environmental impact of the Spanish national hydrological plan on the lower Ebro river and delta. Int. J. Water Resour. Dev. 19, 485–500.
Jalut, G., Esteban Amat, A., Bonnet, L., Gauquelin, T., Fontugne, M., 2000. Holocene climatic changes in the western Mediterranean, from south-east France to south-east Spain. Palaeogeogr. Palaeoclimatol. Palaeoecol. 160, 255–290.
Jalut, G., Dedoubat, J.J., Fontugne, M., Otto, T., 2009. Holocene circum-Mediterranean vegetation changes: climate forcing and human impact. Quat. Int. 200, 4–18.
Jiménez-Moreno, G., Anderson, R., 2012. Holocene vegetation and climate change recorded in alpine bog sediments from the Borreguiles de la Virgen, Sierra Nevada, southern Spain. Quat. Res. 77, 44–53.
Khormali, F., Abtahi, a, Stoops, G., 2006. Micromorphology of calcitic features in highly calcareous soils of Fars Province, Southern Iran. Geoderma 132, 31–46.
Kirchner, H., 1997. La Construcció de l'Espai Pagès a Mayûrqa: les Valls de Bunyola, Orient, Coanegra i Alaró, Universitat de les Illes Balears, Mallorca.
Kirchner, H., 2002. El mapa de los asentamientos rurales andalusíes de la isla de Ibiza. In: Trillo, C. (Ed.), Asentamientos Rurales y Territorio en el Mundo Mediterráneo en Época Medieval. III Jornadas de Arqueología Medieval, Berja, pp. 120–186.
Kirchner, H., 2009. Original design, tribal management and modifications of Medieval hydraulic systems in the Balearic Islands (Spain). World Archaeol. 41, 148–165.
Kovda, I., Mermut, A.R., 2010. Vertic features. In: Stoops, G., Marcelino, V., Mees, F. (Eds.), Interpretation of Micromorphological Features of Soils and Regoliths. Elsevier, Oxford, pp. 109–127.
Krumbein, W.C., 1938. Size frequency distribution of sediments and the normal phi curve. J. Sediment. Petrol. 8, 84–90.
Kuzucuoglu, C., Dörfler, W., Kunesch, S., Goupille, F., 2011. Mid-to late-Holocene climate change in central Turkey: the Tecer Lake record. The Holocene 21, 173–181.
Le Borgne, E., 1955. Susceptibilité magnétique anormal du sol superficial. Ann. Geophys. 11, 399–419.
Le Borgne, E., 1960. Influence du feu sur les proprietes magnetiques du sol et sur celles du schiste et du granite. Ann. Geophys. 16, 159–195.
Lespez, L., Clet-Pellerin, M., Davidson, R., Hermier, G., Carpentier, V., Cador, J.M., 2010. Middle to Late Holocene landscape changes and geoarchaeological implications in the marshes of the Dives estuary (NW France). Quat. Int. 216, 23–40.
Lindbo, D.L., Stolt, M.H., Vepraskas, M.J., 2010. Redoximorphic features. In: Stoops, G., Marcelino, V., Mees, F. (Eds.), Interpretation of Micromorphological Features of Soils and Regoliths. Elsevier, Oxford, pp. 129–147.
Liu, Q., Roberts, A.P., Torrent, J., Horng, C.-S., Larrasoaña, J.C., 2007. What do the HIRM and S-ratio really measure in environmental magnetism? Geochem. Geophys. Geosyst. 8, 1–10.
Liu, Q., Roberts, A.P., Larrasoaña, J.C., Banerjee, S.K., Guyodo, Y., Tauxe, L., Oldfield, F., 2012. Environmental magnetism: principles and applications. Rev. Geophys. 50, 1–50.
Machado, M., Benito, G., Barriendos, M., Rodrigo, F.S., 2011. 500 years of rainfall variability and extreme hydrological events in southeastern Spain drylands. J. Arid Environ. 75, 1244–1253.
Macklin, M.G., Benito, G., Gregory, K.J., Johnstone, E., Lewin, J., Michczyńska, D.J., Soja, R., Starkel, L., Thorndycraft, V.R., 2006. Past hydrological events reflected in the Holocene fluvial record of Europe. Catena 66, 145–154.
Magdaleno, F., Anastasio Fernández, J., Merino, S., 2012. The Ebro River in the 20th century or the ecomorphological transformation of a large and dynamic Mediterranean channel. Earth Surf. Process. Landf. 37, 486–498.

Maher, B.A., 1986. Characterisation of soils by mineral magnetic measurements. Phys. Earth Planet. Inter. 42, 76–92.
Maher, B.A., 1998. Magnetic properties of modern soils and Quaternary loessic paleosols: paleoclimatic implications. Palaeogeogr. Palaeoclimatol. Palaeoecol. 137, 25–54.
Maher, B.A., Taylor, R., 1988. Formation of ultrafine-grained magnetite in soils. Nature 336, 368–370.
Maher, B.A., Thompson, R., 1995. Paleorainfall reconstructions from pedogenic magnetic susceptibility variations in the Chinese loess and paleosols. Quat. Res. 44, 383–391.
Maher, B.A., Alekseev, A., Alekseeva, T., 2002. Variation of soil magnetism across the Russian steppe: its significance for use of soil magnetism as a palaeorainfall proxy. Quat. Sci. Rev. 21, 1571–1576.
Mann, M.E., Zhang, Z., Rutherford, S., Bradley, R.S., Hughes, M.K., Shindell, D., Ammann, C., Faluvegi, G., Ni, F., 2009. Global signatures and dynamical origins of the Little Ice Age and the Medieval Climate Anomaly. Science 326, 1256–1260.
Martín-Chivelet, J., Muñoz-García, M., Edwards, R., Turrero, M.J., Ortega, A.I., 2011. Land surface temperature changes in Northern Iberia since 4000 yr BP, based on $\delta^{13}C$ of speleothems. Glob. Planet. Chang. 77, 1–12.
Martin-Puertas, C., Valero-Garces, B.L., Pilar Mata, M., Gonzalez-Samperiz, P., Bao, R., Moreno, A., Stefanova, V., 2008. Arid and humid phases in southern Spain during the last 4000 years: the Zonar Lake record, Cordoba. The Holocene 18, 907–921.
Martín-Puertas, C., Valero-Garcés, B.L., Brauer, A., Mata, M.P., Delgado-Huertas, A., Dulski, P., 2009. The Iberian-Roman Humid Period (2600–1600 cal yr BP) in the Zoñar Lake varve record (Andalucía, southern Spain). Quat. Res. 71, 108–120.
McCarthy, P.J., Martini, I.P., Leckie, D.A., 1998. Use of micromorphology for palaeoenvironmental interpretation of complex alluvial palaeosols: an example from the Mill Creek Formation (Albian), southwestern Alberta, Canada. Palaeogeogr. Palaeoclimatol. Palaeoecol. 143, 87–110.
Meng, X., Derbyshire, E., Kemp, R., 1997. Origin of the magnetic susceptibility signal in chinese loess. Quat. Sci. Rev. 16, 833–839.
Morellón, M., Valero-Garcés, B., González-Sampériz, P., Vegas-Vilarrúbia, T., Rubio, E., Rieradevall, M., Delgado-Huertas, A., Mata, P., Romero, O., Engstrom, D.R., López-Vicente, M., Navas, A., Soto, J., 2009. Climate changes and human activities recorded in the sediments of Lake Estanya (NE Spain) during the Medieval Warm Period and Little Ice Age. J. Paleolimnol. 46, 423–452.
Moreno, A., Morellón, M., Martín-Puertas, C., Frigola, J., Canals, M., Cacho, I., Corella, J.P., Pérez, A., Belmonte, A., Vegas-Vilarrúbia, T., González-Sampériz, P., Valero-Garcés, B.L., 2011. Was there a common hydrological pattern in the Iberian Peninsula region during the Medieval Climate Anomaly? PAGES News 19, 16–18.
Moreno, A., Pérez, A., Frigola, J., Nieto-Moreno, V., Rodrigo-Gámiz, M., Martrat, B., González-Sampériz, P., Morellón, M., Martín-Puertas, C., Corella, J.P., Belmonte, A., Sancho, C., Cacho, I., Herrera, G., Canals, M., Grimalt, J.O., Jiménez-Espejo, F., Martínez-Ruiz, F., Vegas-Vilarrúbia, T., Valero-Garcés, B.L., 2012. The medieval climate anomaly in the Iberian Peninsula reconstructed from marine and lake records. Quat. Sci. Rev. 4 (3), 16–32.
Morin, J., 1993. Soil crusting and sealing. Soil Tillage in Africa. Needs and Challenges, FAO.
Mullins, C., 1977. Magnetic susceptibility of the soil and its significance in soil science—a review. J. Soil Sci. 28, 223–246.
Navarro, C., 1995. El ma'gil de Liétor: un sistema de terrazas de origen andalusí en activo. I Congreso de Arqueología Peninsular VI, Oporto, pp. 365–378.
Nieto-Moreno, V., Martínez-Ruiz, F., Giralt, S., Jiménez-Espejo, F., Gallego-Torres, D., Rodrigo-Gámiz, M., García-Orellana, J., Ortega-Huertas, M., de Lange, G.J., 2011. Tracking climate variability in the western Mediterranean during the Late Holocene: a multiproxy approach. Clim. Past 7, 1395–1414.
Papayannis, T., Salathé, T. (Eds.), 1999. Mediterranean Wetlands at the Dawn of the 21st Century. MedWet, Tour du Valat.
Provansal, M., Berger, J., Bravard, J., Salvador, P.G., Arnaud-Fassetta, G., Bruneton, H., Vérot-Bourrély, A., 1999. Le régime du Rhône dans l'Antiquité et au Haut Moyen Age. Gallia 56, 13–32.
Puy, A., 2012. Criterios de Construcción de las Huertas Andalusíes. El Caso de Ricote (Murcia, España). (PhD Dissertation) , Universitat Autònoma de Barcelona.
Puy, A., 2014. Land selection for irrigation in al-Andalus (Spain, 8th century A.D.). J. Field Archaeol. 39, 84–100.
Puy, A., Balbo, A.L., 2013. The genesis of irrigated terraces in al-Andalus. A geoarchaeological perspective on intensive agriculture in semi-arid environments (Ricote, Murcia, Spain). J. Arid Environ. 89, 45–56.
Reymer, P.J., Baillie, M.G.L., Bard, E., Bayliss, A., Beck, J.W., Blackwell, P.G., Bronk Ramsey, C., Buck, C.E., Burr, G.S., Edwards, R.L., Friedrich, M., Grootes, P.M., Guilderson, T.P., Hajdas, I., Heaton, T.J., Hogg, A.G., Hughen, K.A., Kaiser, K.F., Kromer, B., McCormac, F.G., Manning, S.W., Reimer, R.W., Richards, D.A., Southon, J.R., Talamo, S., Turney, C.S.M., van der Plicht, J., Wethenmeyer, C., 2009. IntCal09 and Marine09 radiocarbon age calibration curves, 0–50,000 years cal BP. Radiocarbon 51, 1111–1150.
Rigola, J., 2011. Estudi hidrogeològic de la zona del Balneari de Cardó, al municipi de Benifallet. ARDA, Gestió i estudis ambientals. URL http://benifallet.org/uploads/fitxers/projecte%20cardo/2%20estudi%20impacte%20amboental/2602010G_Hidrogeologic%20Cardo.pdf (Accessed 30 January 2014).
Roberts, N., Meadows, M.E., Dodson, J.R., 2001. The history of mediterranean-type environments: climate, culture and landscape. The Holocene 11, 631–634.
Ruiz-Zapata, B., Gil-García, M., de Bustamante, I., 2010. Paleoenvironmental reconstruction of Las Tablas de Daimiel and its evolution during the Quaternary period. In: Sánchez-Carrillo, S., Angeler, D. (Eds.), Ecology of Threatened Semi-arid Wetlands: Long-term Research in Las Tablas de Daimiel. Springer, Dordrecht, pp. 23–40.
Save, S., Buffat, L., Batchelor, C.R., Vannieuwenhuyse, D., Bois, M., Durand, B., 2012. Fleeing from a little bit of water: a very 'un-roman' response to changing environmental constraints. A case study from Monteux, Southern France. eTopoi 3, 113–117.
Schmidt, A., 2007. Archaeology, magnetic methods. In: Gubbins, D., Herrero-Bervera, E. (Eds.), Encyclopedia of Geomagnetism and Paleomagnetism. Springer, New York, pp. 23–31.
Schreiner, M., Frühmann, B., Jembrih-Simbürger, D., Linke, R., 2004. X-rays in art and archaeology—an overview. Powder Diffract. 19, 3–11.
Schwertmann, U., 1988. Occurrence and formation of iron oxides in various pedoenvironments. In: Stucki, J.W., Goodman, B.A., Schwertmann, U. (Eds.), Iron in Soils and Clay Minerals, NATO ASI Series C217. D. Reidel, Dordrecht, pp. 267–308.
Sehgal, J.L., Stoops, G., 1972. Pedogenic calcite accumulation in arid and semi-arid regions of the Indo-Gangetic alluvial plain of Erstwhile Punjab (India)—their morphology and origin. Geoderma 8, 59–72.
Sitjes, E., 2006. Inventario y tipología de sistemas hidráulicos en al-Andalus. Arqueol. Espac. 26, 263–291.
Sitjes, E., 2010. Espacios agrarios y redes de asentamientos andalusíes en Manacor (Mallorca). In: Kirchner, H. (Ed.), Por una Arqueología Agraria: Perspectivas de Investigación sobre Espacios de Cultivo en las Sociedades Medievales Hispánicas. BAR International Series 2062, Oxford, pp. 61–78.
Stoops, G., 2003. Guidelines for Analysis and Description of Soil and Regolith Thin Sections, Soil Society of America, Inc., Madison.
Stoops, G., Marcelino, V., Mees, F. (Eds.), 2010a. Interpretation of Micromorphological Features of Soils and Regoliths. Elsevier, Amsterdam.
Stoops, G., Marcelino, V., Mees, F., 2010b. Micromorphological features and their relation to processes and classification: general guidelines and keys. In: Stoops, G., Marcelino, V., Mees, F. (Eds.), Interpretation of Micromorphological Features of Soils and Regoliths. Elsevier, Oxford, pp. 15–35.
Syvitski, J., 1991. Principles, Methods and Application of Particle Size Analyses, Cambridge University Press, Cambridge.
Taylor, R.M., Maher, B.A., Self, P.G., 1987. Magnetite in soils: I. The synthesis of single-domain and superparamagnetic magnetite. Clay Miner. 22, 411–422.
Taylor, P., Barriendos, M., Rodrigo, F.S., 2006. Study of historical flood events on Spanish rivers using documentary data. Hydrol. Sci. J. 51, 765–783.
Thompson, R., Maher, B.A., 1995. Age models, sediment fluxes and palaeoclimatic reconstructions for the Chinese loess and palaeosol sequences. Geophys. J. Int. 123, 611–622.
Thorndycraft, V., Benito, G., 2006. Late Holocene fluvial chronology of Spain: the role of climatic variability and human impact. Catena 66, 34–41.
Thornthwaite, C.W., 1948. An approach toward a rational classification of climate. Geogr. Rev. 38, 55–94.
Tite, M.S., Mullins, C., 1971. Enhancement of the magnetic susceptibility of soils on archaeological sites. Archaeom 13, 209–221.
Torrent, J., Liu, Q.S., Barrón, V., 2010. Magnetic minerals in Calcic Luvisols (Chromic) developed in a warm Mediterranean region of Spain: origin and paleoenvironmental significance. Geoderma 154, 465–472.
Torró, J., 2007. Vall de Laguar: asentamientos, terrazas de cultivo e irrigación en las montañas del Sarq al-Andalus: un estudio local. Recerques del Museu d'Alcoi, 16, pp. 151–182.
Torró, J., 2010. Tierras ganadas. Aterrazamiento de pendientes y desecación de marjales en la colonixación cristiana del territorio valenciano. In: Kirchner, H. (Ed.), Por una Arqueología Agraria. Perspectivas de Investigación sobre Espacios de Cultivo en las Sociedades Medievales Hispánicas. BAR International Series 2062, Oxford, pp. 157–173.
Tsatskin, A., Gendler, T.S., Heller, F., Ronen, A., 2008. Near-surface paleosols in coastal sands at the outlet of Hadera stream (Israel) in the light of archeology and luminescence chronology. J. Plant Nutr. Soil Sci. 1, 524–532.
Tsatskin, A., Gendler, T.S., Heller, F., Dekman, I., Frey, G.L., 2009. Towards understanding paleosols in Southern Levantine eolianites: integration of micromorphology, environmental magnetism and mineralogy. J. Mt. Sci. 6, 113–124.
Valentin, C., Bresson, L.-M., 1992. Morphology, genesis and classification of surface crusts in loamy and sandy soils. Geoderma 55, 225–245.
Vallve, M., Martin-Vide, J., 1998. Secular climatic oscillations as indicated by catastrophic floods in the spanish mediterranean coastal area (14th–19th centuries). Clim. Chang. 38, 473–491.
van Andel, T.H., Runnels, C., 2005. Karstic wetland dwellers of Middle Palaeolithic Epirus, Greece. J. Field Archaeol. 30, 367–384.
Vannière, B., Bossuet, G., Walter-Simonnet, A.V., Gauthier, E., Barral, P., Petit, C., Buatier, M., Daubigney, A., 2003. Land use change, soil erosion and alluvial dynamic in the lower Doubs Valley over the 1st millennium AD (Neublans, Jura, France). J. Archaeol. Sci. 30, 1283–1299.
Vea, L., 1996. Los Gelida: segmentación clánica bereber y producción de espacios rurales hidráulicos en al-Andalus. Primera aproximación: los riegos de Margarida (Planes de la Baronia, Alacant). In: Cara Barrionuevo, L., Malpica Cuello, A. (Eds.), Agricultura y Regadío en al-Andalus. Coloquio de Historia y Medio Físico 2. Instituto de Estudios Almerienses, Almería, pp. 203–213.
Verdin, P., Berger, J.-F., Lopez-Saez, J.-A., 2001. Contribution of phytolith analysis to the understanding of historic agrosystems in the Rhône mid-Valley (southern France). In: Meunier, J.D., Colin, F. (Eds.), Phytoliths—Applications in Earth Science and Human History. Swets & Zeitlinger B.V., Lisse, pp. 155–172.
Vericat, D., Batalla, R.J., 2006. Sediment transport in a large impounded river: the lower Ebro, NE Iberian Peninsula. Geomorphology 79, 72–92.
Vermoere, M., Bottema, S., Vanhecke, L., Waelkens, M., Paulissen, E., Smets, E., 2002. Palynological evidence for late-Holocene human occupation recorded in two wetlands in SW Turkey. The Holocene 12, 569–584.
Virgili, A., 2001. Ad Detrimentum Yspanie. La Conquesta de Turtusa i la Formació de la Societat Feudal (1148–1200), Universitat Autònoma de Barcelona, Universitat de València, València.

Virgili, A., 2010. Espacios drenados andalusíes y la imposición de las pautas agrarias feudales en el Prado de Tortosa (segunda mitad del siglo XII). In: Kirchner, H. (Ed.), Por una Arqueología Agraria. Perspectivas de Investigación sobre Espacios de Cultivo en las Sociedades Medievales Hispánicas. BAR International Series 2062, Oxford.

Vött, A., Brückner, H., Schriever, A., Luther, J., Handl, M., van der Borg, K., 2006. Holocene paleogeographies of the Palairos coastal plain (Akarnania, Northwest Greece) and their geoarchaeological implications. Geoarchaeol 21, 649–664.

Walkington, H., 2010. Soil science applications in archaeological contexts: a review of key challenges. Earth Sci. Rev. 103, 122–134.

Watson, A.M., 1983. Agricultural Innovation in the Early Islamic World, Cambridge University Press, Cambridge.

Wilhelm, B., Arnaud, F., Sabatier, P., Magand, O., Chapron, E., Courp, T., Tachikawa, K., Fanget, B., Malet, E., Pignol, C., Bard, E., Delannoy, J.J., 2013. Palaeoflood activity and climate change over the last 1400 years recorded by lake sediments in the north-west European Alps. J. Quat. Sci. 28 (2), 189–199.

Zangger, E., 1991. Prehistoric coastal environments in Greece: the vanished landscapes of Dimini Bay and Lake Lerna. J. Field Archaeol. 18, 1–15.